Hydrologic and Water Quality Performance of Bioretention Cells During Plant Senescence

By

Jessica Dhami

BSc, University of Victoria, 2018

A Thesis Submitted in Partial Fulfillment of the

Requirements for the Degree of

MASTER OF APPLIED SCIENCE

In the Department of Mechanical Engineering

©Jessica Dhami, 2022

University of Victoria

All rights reserved. This thesis may not be reproduced in whole or in part, by photocopy or other means, without the permission of the author.

We acknowledge and respect the lək'ʷəŋən peoples on whose traditional territory the University stands, and the Songhees, Esquimalt and W̲SÁNEĆ peoples whose historical relationships with the land continue to this day.

Hydrologic and Water Quality Performance of

Bioretention Cells During Plant Senescence

By

Jessica Dhami

BSc, University of Victoria, 2018

Supervisory Committee

Dr. Caterina Valeo, Supervisor
Department of Mechanical Engineering

Dr. Rustom Bhiladvala, Department Member
Department of Mechanical Engineering

Abstract

Bioretention cells (also known as rain gardens) are a Low Impact Development (LID) method for sustainable stormwater management. An increasingly popular form of urban stormwater infrastructure, bioretention cells use an engineered, vegetated-soil-system to both reduce quantity and enhance quality of stormwater. The ability of bioretention systems to remove common pollutants from urban stormwater runoff, and reduce runoff volume through evapotranspiration, in a temperature climate during plant senescence were assessed in this full scale field-based study. Stormwater run-off simulations were conducted for 5-, 10-, and 25-year return period storm events at a field site in Victoria, British Columbia, Canada. Tests were run on both, a vegetated cell planted with a mix of *Betula nigra, Betula nana*, and *Salix lutea,* and a control cell with turfgrass. Influent and effluent field parameters were recorded for pH and dissolved oxygen (DO), in addition to lab analyses conducted to quantify COD, TN, TON, TP, ortho-phosphate, and TSS removal from the stormwater. Water quality and hydrologic performance were results were compared between the vegetated and control cell using a Wilcoxon Signed Rank Test. In addition, hydrologic results were correlated with daily Evapotranspiration (ET) and meteorological station data using Spearman's Rho Correlation. The vegetated cells were more effective (p value < 0.05) at retention of water volume, DO, COD, and orthophosphate, when compared to the control. Strong correlations (p value < 0.05) were found between the retention of water volume, and each of ET, maximum temperature, average temperature, minimum temperature, and average wind, for only the vegetated cells.

Table of Contents

List of Tables

List of Figures

List of Abbreviations and notation

BOD	Biochemical oxygen demand
BOD_5	five-day biochemical oxygen demand
COD	Chemical oxygen demand
CRD	Capital Regional District
DNA	Deoxyribonucleic Acid
EPDM	Ethylene propylene diene monomer
ET	Evapotranspiration
ET_0	Reference Evapotranspiration
TN	Total nitrogen
TKN	Total Kjeldahl nitrogen
TON	Total organic nitrogen
TP	Total phosphorous
TSS	Total suspended solids
LID	Low Impact Development
M	Meteorological
m	Metre
N	Nitrogen
NO_3-N	Nitrate nitrogen
P	Phosphorous
PO_4^{3-}	Phosphate
PAR	Photosynthetically active radiation
PAH	Polycyclic aromatic hydrocarbons

Acknowledgements

I would like to thank Dr. Caterina Valeo, my supervisor, who supported and guided me throughout my time as a graduate student at UVic offering feedback and providing direction as I conducted my research. In addition to my supervisor, I extend a thank you to Dr. Angus Chu from the University of Calgary. Dr. Chu provided guidance and support with field equipment and laboratory analysis. I would also like to thank Anton Skorobotogatov (PhD candidate) from the University of Calgary, who showed me his field methods and answered my many questions about his work. Another thank you to Alecia LeBlanc, a co-op student with the Bioretention Research Laboratory who assisted with my lab analysis and in many other ways.

1.0 Introduction & Background

1.1 Conventional Stormwater Runoff

As urbanization rates continue to rise, the extent of impervious surface area rises with it. Impervious surfaces include things such as roads, roofs, parking lots, patios, etc. These changes to the natural landscape prevent rain runoff from naturally returning to the hydrological cycle through groundwater recharge (Eckart et al., 2017) and create the need for stormwater infrastructure. Conventional stormwater infrastructure acts to collect and re-direct runoff, where it ultimately terminates at some form of receiving water body or less commonly, a treatment facality. Unfortunately, urban stormwater runoff acts a pathway for contaminants to enter receiving bodies, often causing biological harm and physical changes to the landscape (LeFevre et al., 2015).

When runoff flows along impervious surfaces, it can entrain many forms of pollutants, leading to downstream contamination. Common contaminants found in stormwater include; nutrients, PAH, metals, BOD, COD, pathogens, and TSS. The types and level of each contaminant depend largely on the surrounding land use type and catchment area (Minton, 2005 & Aryal et al., 2010). Physical and biologic effects of urban stormwater runoff are summarized by Hvitved-Jacobsen et al. (2010) and are shown in Table in 1.

Table 1. Overview of physical and biologic effects of urban stormwater runoff (Hvitved-Jacobsen et al., 2010).

Type of effect	**Description**
Physical	• Urban and rural flooding • Erosion by overland flow and natural channels during peak flows • Sediment deposition in receiving bodies
Biologic	• Creation of anoxic environment • Eutrophication due to N and P species, or organics • Metal and organic toxins released to biologic community • Public health risk due to pathogens, and contaminated food (both animal and vegetation)

1.2 Low Impact Development

To remedy the problems that arise with conventional stormwater management, a common practice is the implementation of LID stormwater management tools (sometimes referred to as Green Rainwater Infrastructure). The use of LID technologies is becoming increasingly popular in North America and was first introduced in Vermont, USA in the 1970's with a goal to achieve natural hydrology in urban environments (Barlow et al, 1977, Fletcher et al., 2015). LIDs are a group of tools used to supplement the conventional stormwater infrastructure by allowing water to return naturally to the hydrological cycle through promoting infiltration and evapotranspiration (ET) (Liu et al., 2014a, Li & Davis, 2009). Common LIDs include bioretention cells (otherwise known as rain gardens), green roofs, and porous pavers. In addition to capturing peak flows and promoting ET, LIDs can aid in reducing the heat island effect, add green space in urban areas and enhance effluent water quality (Liu et al., 2014a, Dunn, 2010).

1.3 Bioretention Cells Overview

Bioretention cells are a common and widely useful LID stormwater management tool. Maintaining the goals of infiltration and ET, bioretention cells are a combination of engineered soil media and dense vegetation strategically designed to meet site-specific runoff attenuation goals. The basic concept of bioretention is capture of stormwater runoff, followed by a delayed release to the storm drain system and/or losses by ET (Winogradoff, 2002). Both variations act to reduce the peak flows and reduce outflow volumes. In addition to the hydrologic capabilities of bioretention cells, they act as primary treatment for common stormwater pollutants. This

occurs via plant uptake or adsorption to plant root systems and soil particles (Hsieh & Davis, 2003, Hsieh & Davis, 2005, Davis et al., 2006, Winogradoff, 2002). Bioretention cells are highly customizable to meet site needs, however they all have a set of common features that may include some, if not all of the following: a runoff inlet, ponding area, dense vegetation, mulch layer, engineering soil media, gravel drainage layer, and outflow drain (Kim et al., 2003). A basic bioretention cell is presented in figure 1.

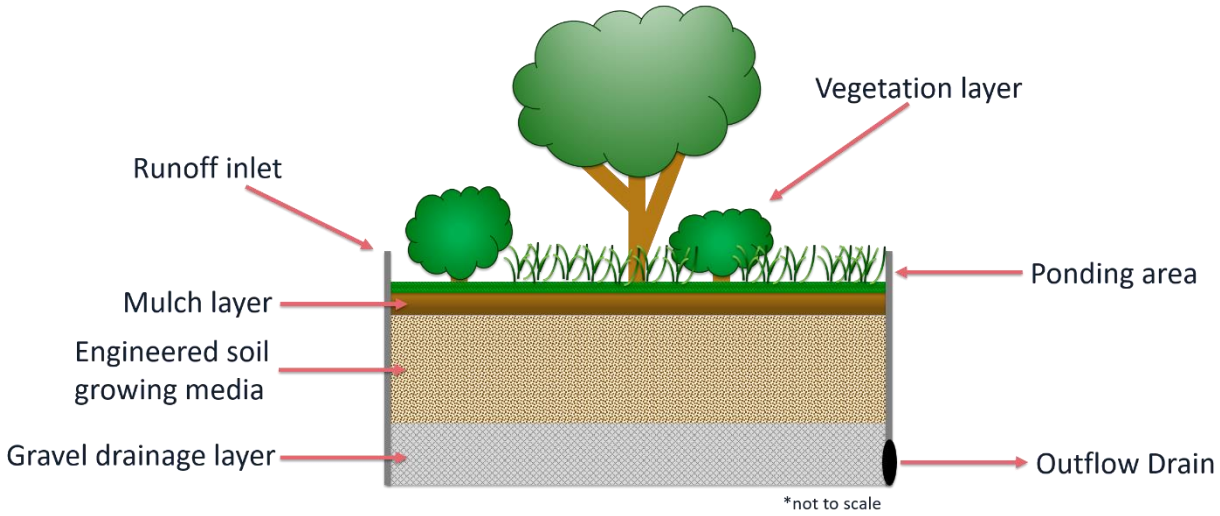

Figure 1. Basic bioretention cell design.

1.4 Bioretention Performance

It has been known since the early 2000's that bioretention cells are effective at reducing peak flows, effluent volumes, and reducing time of concentration (EPA 2000; Skorobogatov et al., 2020). The hydrologic performance of these systems is largely a factor of design, location, and peak flow (Li et al., 2019). Quantity of runoff volume reduction, ET, and infiltration are all common parameters to characterize effectiveness of a bioretention system (Skorobogatov et al., 2020). In a review by Liu et al, (2014b) it was determined that overall bioretention can

reduce time of concentration from five minutes to several hours based on site design and flow rate. In the same study Liu et al, (2014b) determined that runoff outflow volume could be reduced by 19%, attributed to ET. Longevity of hydrologic performance of bioretention systems was studied by Lucke and Nichols (2015) on 10-year old bioretention cells. After 10-years of use, bioretention cells reduced the peak outflow volume by 79.5 – 93.6%; however, it was noted that the lowest reductions were correlated to a pre-saturated basin (Lucke & Nichols, 2015). A study of bioretention performance at three sites in varying climates found 83 - 96% reduction in peak runoff was possible for small storm events, but as the events became larger in volume, the results were reduced to as little as 14% (Hatt et al., 2009). Although the varying climates were mentioned by Hatt et al, (2009) there was a lack of discussion or comparison of results between the three climatic zones. Seasonality plays a role in the hydrologic capabilities of bioretention systems. Bonneau et al, (2020) conducted a study on bioretention systems over a 3-year period in Melbourne, Australia and found that catchment runoff was reduced by 35 – 45% in volume, however ability to reduce outflow volumes was significantly lower during the winter months due to basin saturation.

Along with hydrologic benefits discussed above, bioretention can play a role in water quality enhancement. Receiving water bodies are at risk of eutrophication due to nutrient pollutants, mainly Nitrogen (N) and Phosphorus (P) species, resulting in ecosystem imbalances and harmful algal blooms (Yang & Lusk, 2018). N and P species in stormwater are found both in dissolved or particle form, and can enter the environment through several mechanisms including atmospheric deposition, chemical fertilizers, organic leaching, and sanitary sewer overflows (Yang & Lusk, 2018). Many full scale, field studies have been conducted on the ability

of bioretention cells to remove nutrient pollutants in runoff water, with varying results. Hatt et al. (2009) found a general reduction in Total Nitrogen (TN), the magnitude of which varied with the vegetation type, however some tests revealed leaching. In the same study, nitrate was found to leach into the effluent water, where Total Phosphorus (TP) was consistently removed from the stormwater. These results are concurrent with several other more recent studies (Davis et al., 2006; Lucke & Nichols, 2015; Bonneau, J. et al., 2020).

TSS is another common stormwater pollutant which is often used as an overall water quality indicator for other harmful pollutants, which may bind to the entrained silt or sediment. In receiving bodies, TSS can cause harm by clogging the gills of fish, attenuating light for photosynthesizers, or smothering other biologic organisms. The presences of TSS (as with other pollutants) is largely dependent on the land use surrounding the catchment area, but most commonly introduced by construction activities and flow over impervious surfaces (Minton, 2005, Li & Davis, 2008). Bioretention cells can act as a bio filter to remove TSS from stormwater runoff. They have proven to reduce TSS loads by 52 - 97% in recent studies (Bonneau, J. et al., 2020, Davis, 2007, Hatt et al., 2009). It has been shown that bioretention cells may leach TSS during initial use but will reach a point of maturity with constant TSS concentrations in the effluent water (Hatt et al., 2008).

Some work has been done in the field of long-term bioretention performance. In general, it's found that removal of TN, nitrogen species, and TP remains high in the long term, however, the hydrological capacities and TSS removal reduce over time (Lopez-Ponnada et al., 2020; Shrestha et al., 2018; Wang et al., 2021).

1.5 Plant Senescence

Plant or leaf senescence is a lifecycle stage of deciduous plants when the leaves begin to die, following the growing season. Senescence in vegetation is highly complex and can be characterized by degradation of chlorophyll, re-location of nutrients within the plant structure, and hormone levels (Gulfishan et al., 2018). In deciduous plants, leaf senescence serves the purpose of preservation during periods of low solar insolation (i.e. fall and winter), by reducing the vegetation biomass, less energy is required for survival (Leopold, 1961). Senescence is followed by abscission, when the necrotic plant tissue is dropped from the main structure, or in the case of deciduous trees, when the leaves fall. For the purpose of this study the senescence period was defined by visual degradation of chlorophyll, simply by observation of the leaves changing from green to brown.

1.6 General Objectives and Thesis Layout

The literature is lacking studies on the long term performance changes due to the vegetated component of bioretention cells. Very little information is available around changes in bioretention performance with the vegetation's natural lifecycle and seasonal variations. This lack of knowledge hinders widespread and accepted implementation of bioretention cells in Canadian climates in which senescence is a part of the vegetation's annual cycle. The overall objectives of this thesis are to examine the hydrological and water quality performance of bioretention cells during plant senescence and abscission. This Chapter is followed by the literature review on bioretention cell performance related to vegetation in Chapter 2, detailed objectives in Chapter 3, experimental methods for this study in Chapter 4, results are presented

in Chapter 5, and discussion of results, conclusions of the study, and recommendations for future work are given in Chapter 6.

2.0 Literature Review

2.1 Role of Vegetation in Bioretention Cells

Plants preform two roles in bioretention systems, (1) uptake of nutrients from the soil, and (2) recycle water through transpiration.

In the recent literature several authors have compared the role vegetation in removing nutrient pollutants (Dagenais et al., 2018; Rycewia-Borecki et al., 2017; Vijayaraghavan et al., 2021), results are mixed. In a greenhouse controlled study Rycewica-Borecki et al. (2017) compared planted systems for removal of TP and TN by plant uptake, via plant tissue analysis. Minor differences were found across plant type; however, results showed all vegetation types effective in the uptake of nutrient pollutants. Dagenais et al. (2018) reports similar positive results for nutrient removal with the presence of vegetation, but does make a point to attribute the magnitude to root structure and growth rate. Similar results have been found for nitrate and ammonia in multiple species of aquatic plants (Zuo et al., 2020). However, in a recent review by Vijayaraghavan et al. (2021), the authors point to the mixed the results of evidence for vegetation aiding in removal of TP and TN, highlighting recent studies have showed removal of TP with the presence of vegetation in bioretention systems can range from 4 to 99%.

TSS is a common stormwater pollutant and often considered in the design and study of bioretention cells. The mechanism of TSS removal in bioretention systems is generally capture by the soil filter, which over time become clogged (Hatt et al., 2009). TSS is not a pollutant used as a food source for vegetation, however Hatt et al. (2009) believes that root growth and structure change can loosen the soil, aiding in permeability, and in turn unclogging the soil

media filter. On the other hand, Barrett et al. (2013) compared the removal of TSS in bioretention cells between vegetated and grass cells, to find very little difference (<10 %) between the two. Similar results were reported by Dagenais et al. (2018).

Through a vigorous literature search the only study found to date directly comparing the influence of vegetation on ET in bioretention systems was completed by Nocco et al. (2016). This group compared turf grass, shrub, prairie, and bare soil, in field-scale bioretention cells. The presence of vegetation increased ET by four times, but only for some vegetation types (Nocco et al., 2016). A review by Berland et al. (2017) points out the lack of research quantifying ET due to vegetation in bioretention systems, but does use basic hydrological principles, ET, and land use studies to suggest that treed vegetation would greatly increase ET compared to turfgrass.

The relationship between plant roots, soil structure, and macropores is explored in a review by Skorobotogv et al. (2020), where its shown at macropore size and orientation greatly affects how pollutants are retained by soils in bioretention systems and how water flows. It is recognized that plant – soil interaction plays a role in both water quality and hydrologic performance however it is not the focus of this study.

2.2 Seasonal Influence on Bioretention Performance

Limited studies have been conducted to investigate the role of seasonal influence on bioretention systems. Several groups have studied and prepared guidance documents on vegetation selection for different climate regions and long term efficacy but only consider the

overall climate and do not explore the scale of seasonal changes (Goh et al., 2019; Lopez-Ponnada et al., 2020; Lucke et al., 2015; Lucke et al., 2017; Shrestha et al., 2018; Wang et al., 2020).

The relationship between treed vegetation and ET in bioretention cells has been explored with a focus on balancing the tradeoff of high ET and drought stress (Szota et al., 2018). Szota et al. (2018) quantified this ET – drought risk relationship across 20 different tree species to determine the best species for contributing to ET while also showing resiliency in drought conditions. However, Szota et al. (2018) only simulated well-watered and drought conditions with watering inside a climate controlled greenhouse, excluding the meteorological changes between the two seasonal conditions. Nocco et al., (2016) ran field-scale bioretention experiments comparing the hydrological abilities and N cycling on turfgrass, shrub, prairie, and bare soil, in the mid-west United States, through July, August, and October. However, the results are not greatly explored from the lens of the changing season, only that of the vegetation media.

Very few studies have directly investigated changes in bioretention performance with seasonal variation. Some work has been done in the area of “dual-mode” biofilters, where the bioretention systems are irrigated with grey water during periods of drought (Barron et al., 2020). Barron et al. (2020) found pollutant removal to be similar between stormwater and greywater, suggesting greywater in dry periods is a practical solution for maintenance of bioretention systems. However, this does not explore how bioretention systems would naturally withstand drought conditions with seasonal change. Another study by Goor et al.

(2021) looks at the seasonal performance of bioretention systems' ability to retain phosphorous specifically in cold climates with the influence of road de-icing salt in the runoff. Seasonal effects on bioretention performance in tropical climates has been studied by Hermawan et al. (2020), where the group simulates wet and dry periods on bioretention systems and asses the nutrient removal, heavy metal removal, and drought resistance.

3.0 Objectives

3.1 Gaps in Knowledge

Research groups have only recently begun to explore how seasonal changes affect bioretention performance. Studies have been conducted in tropical climates, where intense rains are followed with intense dry periods. The selection of drought resistant vegetation that can maintain ET in wet periods is know well studied, and the field is beginning to explore alternate irrigation sources to recycle water during periods of drought. Work has been done in the field of the cold climate bioretention systems, and how partially or fully frozen environments affect performance. Little to no research has been conducted in temperate climate regions, during plant senescence when vegetation is dying off and nutrient uptake is likely reduced. This study will conduct experiments during the plant senescence period and compare to the literature to explore the potential seasonal effect on both nutrient uptake and hydrological capacity.

The role of vegetation in bioretention cells is becoming more widely understood, and several versions of guidelines exist to aid a designing party in the selection of vegetation type. However, very few studies use a grass or soil control to compare to the results of vegetated cells. In the majority of the literature on vegetation in bioretention cells, focus is given to comparing across vegetation types. Therefore, a solid understanding on if vegetation in bioretention cells has a preferred influence water quality and hydrological performance compared to grassed cells does not exist. This study will compare the results of vegetated bioretention cells and grass bioretention cells to further this area of research.

3.2 Thesis Objectives

The Specific objectives of this thesis are:

1. Determine the ability of Bioretention cells to remove nutrient pollutants and TSS during plant senescence and abscission;
2. Determine the hydrologic ability of bioretention cells to reduce peak runoff loads through evapotranspiration during plant senescence and abscission, and;
3. Investigate the role of vegetation in both the water quality and hydrologic performance of bioretention cells.

4.0 Methods & Calculations

4.1 Site Description

The study site is located on the west coast of Canada at the University of Victoria on Vancouver Island, British Columbia. This is a temperate climate region where the temperature is largely influenced by the sea surface. The site consists of four, 2 m $\times$ 2 m in area bioretention cells, ranging from 1.05 – 1.21m in depth. There is a 2% grade underdrain connecting all four cells which flows into a single sediment trap to capture the effluent water. Each cell is completely lined with an EPDM impermeable pond liner. From bottom to top, the bioretention soil media layers consist of: 200 – 290mm of 40mm diameter drainage rock; a geotextile (Propex 351); a 750 – 950mm thick rooting zone made up of 30% compost and 70% growing media (silty sand); a 25mm mulch layer; and a layer of vegetation. Site plans can be found in Appendix A. Two cells on the site were covered in grass to act as a control and two cells contained a mix of Betula nigra (River Birch), Betula nana (Dwarf Birch), and Salix lutea (Yellow Willow). The plant configuration and cell layout can be seen in figure 2. The bioretention cells were built in 2014 by the bioretention research laboratory and have not had any significant testing conducted on them prior to this study.

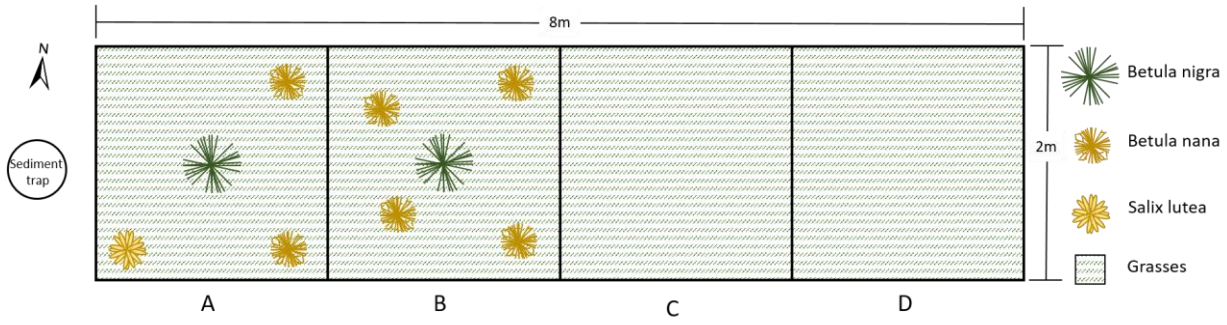

Figure 2. Layout at bioretention research site, Victoria BC.

The site is outfitted with 6 Zentra Utility soil moisture sensors, and a HOBO U30 Meteorological station, both with internal data loggers. The soil moisture sensors are installed in cells A - C at depths of 20 and 40cm, details can be seen in Table 2. The meteorological station is equipped to record; rainfall, wind speed, gust speed, photosynthetically active radiation (PAR), pressure, temperature, and relative humidity.

Table 2. Soil moisture sensor configuration.

Port	Cell	Depth (cm)
1	C	40
2	C	20
3	B	40
4	B	20
5	A	40
6	A	20

4.2 Return Volume Calculations

At the time of this study, the District of Saanich (where the University of Victoria exists) did not have any design guidelines for low impact development. In addition, the freeboard height on the study site does not allow for large volumes of ponding water (i.e. one in 200 year rainfall event, or entire catchment area volumes). Therefore test volumes corresponding to 5-, 10-, and 25-year return period rainfall events, were calculated by a frequency analysis was run on historical rainfall data and a non-linear least squares regression was applied to the intensity curve. Historical daily meteorological data was obtained from Environment Canada (Environment Canada, 2019A) for the weather station located on the University of Victoria campus (station: "Victoria University CS British Columbia"). Available data covered the years 1992 to 2019 and all the data that was available data was used. The raw data was subset into annual senescence periods and a seasonal maximum was extracted for each year. A frequency analysis was completed on the data to calculate the given return period for the seasonal total precipitation. Equation A1 was used, where p is this probability of occurrence, T is the return period, n is the rank, and m is the number of observations.

Equation 1

$$p = \frac{1}{T} = \frac{n}{m+1}$$

The data was plotted with rainfall intensity in mm/day (per square metre) against return period and a non-linear least squares regression was run to fit a curve to the data. The logarithmic equation 2 was used, where R is the rainfall intensity, T is the return period, and both a (19.07) and $b(20.14)$ are coefficients of the regression. The results can be seen in

figure 3 and calculated rainfall intensity in Table 2. To convert rainfall intensity to test volumes (*V*), they were multiplied by the surface area of the cell (*A*) to represent the volume of rain that would fall on the cell in a day. This is shown in equation 3, and final test volumes per one cell are given in Table 3. The python code used to complete these calculations is given in Appendix B.

Equation 2

$$R = aln(T) + b$$

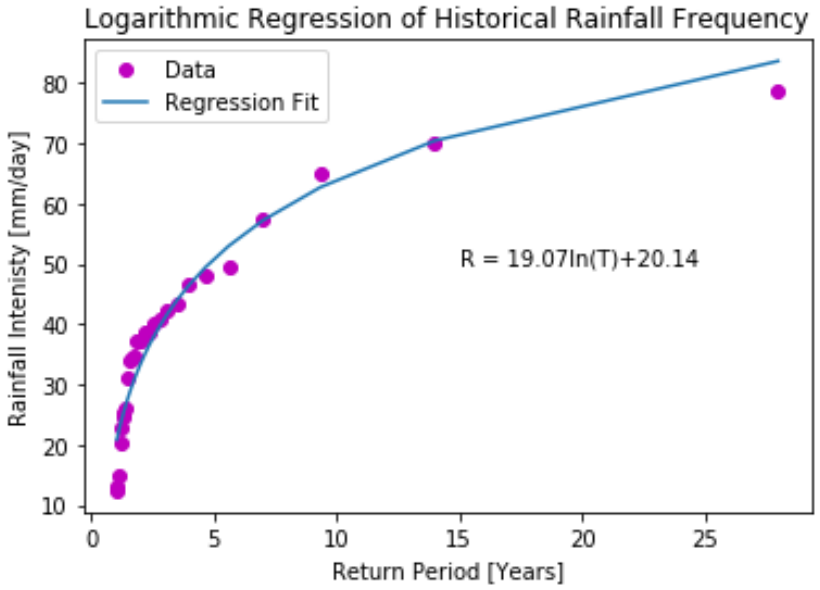

Figure 3. Best fit line resulting from fitting a logarithmic function to the rainfall intensity data.

Equation 4

$$V = A * R$$

Table 3. 5-, 10-, and 25-year daily rainfall intensities from linear regression and return period test volumes per one cell.

RETURN PERIOD [YEARS]	RAINFALL INTENSITY [MM/DAY]	FINAL TEST VOLUME [L]
25	80	320
10	65	260
5	50	200

4.3 Field Methods

A total of 18 individual, full-scale bioretention rainfall runoff simulations were completed at the site between August 15th and October 7th, 2020. The beginning of plant senescence was confirmed by the observation of leaf yellowing/browning (photo 1) and the study period ended before the trees were in complete dormancy (photo 2).

Photo 1. Beginning of senescence 14-08-2020.

Photo 2. Vegetation in senescence/abscission 07-10-2020.

Due to the short duration of the plant senescence period and the time required between test events, the cells A and B were tested together as one unit and cells C and were tested together as one unit. This resulted in one 2 x 4m (in surface area) bioretention cell and one 2 x 4m (in surface area) control cell for the purpose of this study. Three rainfall runoff

volumes were tested: 400, 520, and 640L, corresponding to 5- , 10-, and 25-year storm events for the region, respectively. Each return volume was tested three times on the bioretention cells (cells A and B, figure 2) and three times on the control cells (cells C and D, figure 2). Each test was assigned a test ID based on return period, bioretention/control, and test number.

In the field, pre-weighed lab grade chemicals and sediment were mixed with the correct volume of water to simulate stormwater runoff. The water was applied to the cells, both influent and effluent water samples were collected for lab analysis. In the field, influent and effluent water were monitored for field parameters (DO and pH). Test events were run from weeks to as little as several hours apart based on the event size, time for effluent water flow to terminate, and weather. The test event schedule is shown in Table 4.

Table 4. Field test schedule, test ID, return period, and test volume.

Date (yyyy-mm-dd)	Test ID	Return Period (-yr)	Test Volume (L)
2020-08-15	5-B-1	5	400
2020-08-17	5-C-1	5	400
2020-09-11	25-B-1	25	640
2020-09-12	25-C-1	25	640
2020-09-15	10-B-1	10	520
2020-09-15	10-C-1	10	520
2020-09-17	5-B-2	5	400
2020-09-21	5-C-2	5	400
2020-09-21	10-B-2	10	520
2020-09-22	10-C-2	10	520
2020-09-22	25-B-2	25	640
2020-09-29	25-C-2	25	640
2020-09-30	5-B-3	55	400
2020-10-01	25-B-3	25	640
2020-10-02	10-C-3	10	520
2020-10-05	10-B-3	10	520
2020-10-06	25-C-3	25	640
2020-10-07	5-C-3	5	400

4.3.1 Field Procedure

The field test procedure was conducted as follows:

1. To simulate nutrient and TSS pollutants in storm water, prior to field testing, lab grade ammonium chloride, monobasic potassium phosphate, dibasic potassium phosphate, and sand and sediment sieved down to 75µm was measured using an analytical balance. The nutrients were measured to create concentrations mid-range of the lab test ranges, and the TSS was measured to create concentrations equal to the average CRDS TSS concentration in stormwater (CRD, 2019). Monobasic and Dibasic potassium phosphate were mixed at equal molar concentrations to maintain a neutral pH.
2. In the field, the correct volume of water was measured in to a large tank with graduated markings. The nutrient pollutants were added to the tank and two utility pumps were used to circulate the water for a minimum of twenty minutes, to allow for the chemicals to dissolve (photo 3). A YSI was deployed in the graduated tank, temperature, DO, and pH were recorded.

Photo 3. Graduated tank used to measure test volumes and mix nutrient pollutants.

3. The simulated influent stormwater was then applied to the cells using the utility pumps and a perforated hose (photo 4). The TSS was mixed with the influent water in a Nalgene bottle and applied to the cells in the areas with the most ponding. Attempts were made to mix the TSS in the gradated tank, however issues arose with keeping the particles suspended after the mixing period.

Photo 4. Perforated hose and TSS being applied to the cells.

4. A 500ml sample of the influent water was collected in a clean Nalgene bottle, by compositing the water being applied to both cells.
5. As effluent water began draining into the sediment trap a YSI was used to record temperature, DO, and pH (photo 5). Effluent was then pumped into a smaller graduated tank to record effluent volume and collect a 500ml sample (photo 6). Influent and

effluent samples were stored in the field in a cooler with ice, then transferred to a refrigerator in the bioretention research laboratory for storage prior to analysis.

6. A shop vac was used to extract all water draining into the sediment trap and was added to the total effluent volume. This was repeated until there was no more visible water draining from the outflow pipe, this time frame varied from several hours to multiple days.

Photo 5. Effluent draining into sediment trap and YSI deployed

Photo 6. Effluent water pumping into small graduated tank.

4.3.2 LAI Data

Leaf Area Index (LAI) data was collected intermittently thought the study period. Data was collected using a METER Group® LP-80 Photosynthetically Active Radiation and Leaf Area Index Meter. LAI measurements were recorded by placing the LAI beneath the canopy until a record was collected. This was completed between the hours 11:00am and 1:00pm to catch the sun as it passes through its highest angle. LAI is a unitless ratio of the area of leaves per area of soil surface, and can be used to aid in the definition of plant senescence or senescence based on canopy cover.

4.4 Lab Analytical Procedures

All chemical analyses were conducted at the Bioretention Research Laboratory at the University of Victoria, with the exception of BOD_5. Analyses for COD, NH_3 - N, TN, TkN, total P, and ortho PO_4^{3-} were conducted using commercially available HACH® brand test kits. The methods used were HACH® 8000, 831, 10208, 10242, 8190, and 8048, respectively. Detailed instructions for each method are available at hach.com. Three water samples were sent to Bureau Veritas lab for BOD_5 analysis. Total Organic Nitrogen was calculated by subtracting Nitrogen as Nitrate from Total Kjeldahl Nitrogen ($TKN - (NH_3 - N) = TON$).

TSS was analyzed by vacuum filtration. A 1.5µm glass fiber filter was weighed using an analytical balance, then placed on the vacuum filtration system. A known volume of sample was run through the vacuum and collected on the filter. The filter was then placed in an oven at approximately 105 °C for a minimum of 12 hours to evaporate any water remaining on the filter. The filter was then allowed to cool inside a desiccator at room temperature, then weighed again. A difference was calculated from the original filter mass to find the mass of solids, this was divided by the volume of sample used and converted to units of milligrams per litre (equation 4).

Equation 4

$$TSS\ (mg/L) = \frac{Final\ mass\ (mg) - Initial\ mass\ (mg)}{Volume\ of\ filtered\ sample\ (L)}$$

Concentrations for each contaminaent and water quality parameter is given per test Table 5 below.

Table 5. Concentration of contaminants and field parameters in influent water. Note: "-" indicates inconclusive results.

	Field		Lab					
Test ID	**DO (mg/L)**	**pH**	**COD (mg/L)**	**Total P (mg/L)**	**Ortho PO_4^{3-} (mg/L)**	**TSS (mg/L)**	**TN (mg/L)**	**TON (mg/L)**
5-B-1	8.74	8.58	5.0	1.45	1.34	6.00	14.50	12.99
5-B-2	8.38	6.98	<3.0	1.28	1.26	31.00	4.37	0.33
5-B-3	8.78	6.39	5.8	1.34	1.20	20.07	3.45	0.00
5-C-1	9.07	8.29	<3.0	1.59	1.49	-	15.20	14.52
5-C-2	8.20	7.00	<3.0	1.27	1.23	0.00	3.47	0.09
5-C-3	9.06	9.73	3.7	1.25	1.16	18.01	3.06	0.00
10-B-1	8.94	7.65	<3.0	1.39	1.33	25.00	3.04	0.00
10-B-2	8.58	7.43	<3.0	1.37	1.36	49.77	4.06	0.80
10-B-3	9.79	9.39	<3.0	1.30	1.24	18.07	3.04	0.00
10-C-1	8.61	6.54	3.7	1.45	1.24	5.00	3.73	0.47
10-C-2	8.82	7.83	<3.0	1.41	1.37	50.48	3.49	0.27
10-C-3	9.01	9.84	<3.0	1.23	1.11	18.03	2.89	0.00
25-B-1	8.88	8.59	<3.0	2.03	1.13	-	11.95	11.32
25-B-2	8.75	7.80	<3.0	1.33	1.31	55.96	3.11	0.00
25-B-3	8.95	8.05	<3.0	1.49	1.32	17.90	2.27	0.00
25-C-1	8.30	8.34	<3.0	2.08	1.08	2.50	12.13	11.37
25-C-2	9.40	8.74	<3.0	1.86	1.16	50.06	3.09	0.00
25-C-3	9.28	9.71	<3.0	1.34	1.33	15.07	2.95	0.00

4.5 Data Analysis

4.5.1 Statistical Analysis

A mass balance for water volumes, concentrations of each chemical species and field parameter were calculated to obtain a dataset for analysis. Equation 5 displays how a mass balance was calculated for the water volumes, the same formula was used for the chemical species.

Equation 5

$$\Delta water\ volume\ (L) = Effluent\ volume\ (L) - Influent\ volume\ (L)$$

To normalize the data a percent change of each variable was calculated for the influent and effluent pairs, this provides the water retention rate and pollutant removal efficiency for each test. Equation 6 shows an example of how this was done for water volume. A simple average change was calculated for each variable in the bioretention cells and control cells, for comparison.

Equation 6

$$\%\Delta water\ volume = \frac{Effluent\ volume\ (L) - Influent\ volume\ (L)}{Influent\ volume\ (L)} \times 100$$

The bioretention and control mass balance data were paired by return volume and test number (i.e. 5-B-1 was paired with 5-C-1) and a Wilcoxon Signed Rank Test was run on the paired data. The Wilcoxon Signed Rank Test is a non-parametric test used to compare related data pairs, where the null hypothesis suggests the median of differences between the paired sets of data equals zero. The test was run using IBM® SPSS statistics software package with a significance level of 0.05, and a confidence interval of 95.0%. The output from SPSS can be found in Appendix C.

Correlation coefficients were calculated using Spearman's Rho Correlation for non-parametric data. A two-tailed correlation value was calculated between the water retention rate and each of the MET station parameters (daily maximum, daily average, and daily minimum), as well as the daily ET_0 data (see section 4.5.2 below); both from the same day corresponding to the field test for the water volume data. A p-value was calculated for each correlation, and significance values less than 5 %, and less than 1 % were highlighted. The

Spearman's Rho test was run IBM® SPSS statistics software package. The output from SPSS can be found in Appendix C.

4.5.2 Daily ET Determination

Daily reference ET (ET_0) for a grass surface was calculated using the Food and Agriculture Organization of the United Nation's (FAO) ET_0 Calculator (FAO, 2009). FAO incorporates the MET station data, study site location, and study site elevation data to calculate daily ET_0 using the FAO Penman-Monteith equation (FAO, 1998); a FAO modified Penman-Monteith equation (Equation 7). A full derivation of the equation can be found in FAO's documentation (FAO, 1998). Where; ET reference evapotranspiration [mm/day], R_n net radiation at the crop surface [MJ/m^{2}day], G soil heat flux density [MJ/m^{2}day], T air temperature at 2 m height [°C], u_2 wind speed at 2 m height [m/s], e_s saturation vapour pressure [kPa], e_a actual vapour pressure [kPa], $e_s - e_a$ saturation vapour pressure deficit [kPa], D slope vapour pressure curve [kPa/°C], and g psychrometric constant [kPa/°C].

Equation 7

$$ET_0 = \frac{0.408\Delta(R_n - G) + \frac{900}{T + 273}u_2(e_s - e_a)}{\Delta + \gamma(1 + 0.34u_2)}$$

Reference ET was converted to crop ET (ET_C) for the vegetated bioretention cells using the conversion given in equation 8 (FAO, 1998). Where; ET_0 reference ET [mm/day], K_c crop coefficient (unit-less), and ET_C crop ET [mm/day]. The crop coefficient was determined using equation 9 which gives Kc as a function of LAI (Jia & Wang, 2021). Jia and Wang (2021)

developed this relationship for apple trees, however due to the similarities in structure and size it can be applied to the birch trees present in this study.

Equation 8

$$ET_C = K_C ET_0$$

Equation 9

$$K_c = 0.1141e^{1.0665LAI}$$

4.5.3 Field Capacity and Permanent Wilting Point Determination

Following saturation, field capacity is the soil's water content after initial gravity drainage has stopped. Permanent wilting point is the state when evapotranspiration has occurred and the water content in the soil is too low for uptake by plants. Figure 4 (FAO, 1985) provides a visual example of a) saturation, b) field capacity, and c) permanent witling point.

Field capacity and permanent wilting point were determined from the soil moisture data at 20 cm depths (rooting zone) based on the above FAO (1985) definitions and examples given from the soil moisture sensor manufacturer (Campbell, n.d.). Due to the season of the study period and the frequency of test events, it is likely that the true field capacity and wilting point were not reached between test events. Therefore, these values were determined from the first test with soil moisture data: September 11 for the vegetated bioretention cells, and September 12 for the control cells. Further, based on the nature of the non-controlled environment and exposure to atmospheric conditions, what appears to be permanent wilting point in the soil moisture data will here on be referred to as antecedent moisture content. Antecedent moisture

content was determined as the soil moisture value immediately before the first test, and field capacity as the point where the soil moisture curve begins to flatten.

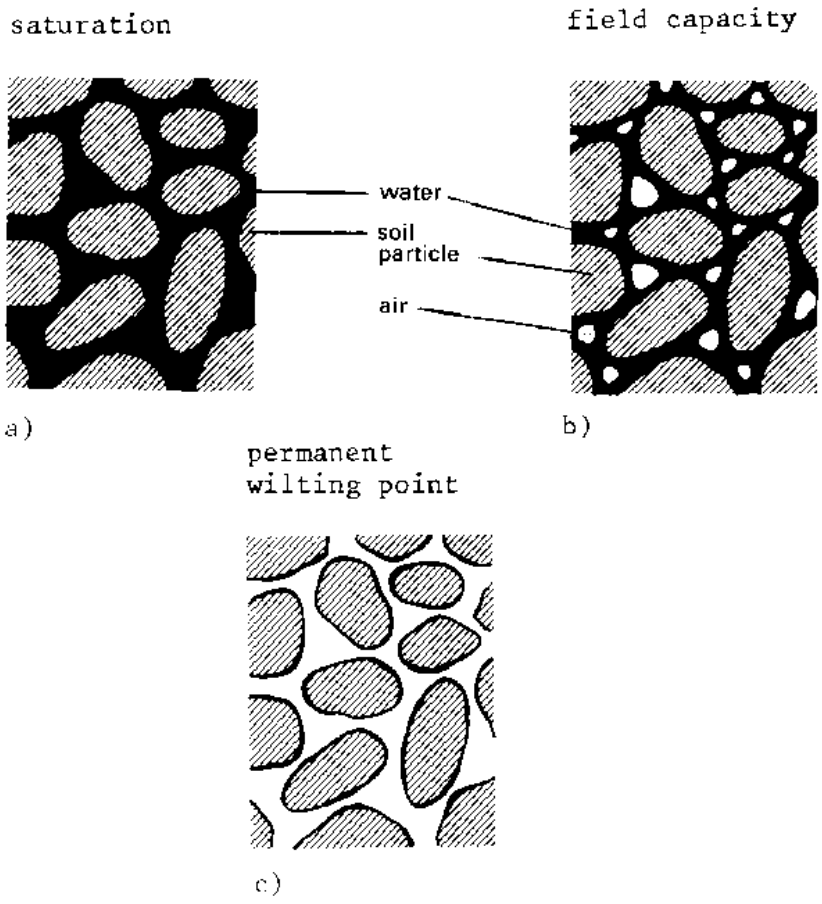

Figure 4. Soil saturation, field capacity, and permanent wilting point (FAO, 1985).

5.0 Results

5.1 Mass Balance and Paired Tests

The change in each parameter (mass balance) by test is given in Table 6, as well as the normalized percent change in 8. Two TSS results are omitted due to lab errors. Table 8 provides the average change for each parameter in the bioretention cells and the control cells, to compare the overall performance of the two systems. Results from the Wilcoxon Signed Rank Test consist of a p value (Table 8) which indicate whether the null hypothesis should be rejected. In the case of this test, the null hypothesis states "the median of differences between the paired sets of data equals zero". Therefore, in cases where the null hypothesis is rejected, the performance of the bioretention cells was statically difference than the performance of the control cells. Of the ten parameters included in the statistical analysis, five resulted in p values which indicated the null hypothesis could be rejected (Table 8).

Table 6. Mass balance results for each parameter and test.

Test ID	Δ Volume (L)	Δ DO (mg/L)	Δ pH	Δ COD (mg/L)	Δ Total P (mg/L)	Δ Ortho PO_4^{3-} (mg/L)	Δ TSS (mg/L)	Δ TN (mg/L)	Δ TON (mg/L)
5-B-1	-295.00	-4.40	-0.42	26.5	-0.74	-0.85	21.00	-12.26	-12.59
5-B-2	-195.00	-1.73	-1.11	66.4	-0.37	-0.74	-20.00	3.96	0.76
5-B-3	-95	-3.16	1.65	67.7	0.45	-0.02	10.93	2.79	1.47
5-C-1	-255	-1.98	0.46	60.7	-0.44	-0.70	-	-8.80	-14.52
5-C-2	-133	-0.10	-0.94	76.1	0.09	-0.25	4.00	6.87	0.91
5-C-3	-48.5	-2.76	-0.74	73.9	-0.40	-0.40	-10.01	0.96	0.00
10-B-1	-355	-1.99	-1.23	75.7	-0.79	-0.75	-9.00	2.41	0.00
10-B-2	-218	-1.63	-0.95	67.1	-0.52	-0.71	-43.77	3.99	-0.01
10-B-3	-110	-4.81	-1.10	64.3	-0.61	-0.35	-15.07	2.64	0.10
10-C-1	-307	-0.73	-0.25	92.2	0.03	-0.31	22.00	9.10	0.77
10-C-2	-150	-1.78	-1.03	84.6	-0.15	-0.51	-45.48	6.96	0.38
10-C-3	-20.5	-2.46	-1.23	66.9	-0.31	-0.31	-14.03	1.06	0.00

25-B-1	-425	-0.68	-0.50	63.1	-0.82	-0.40	-	-6.88	-10.17
25-B-2	-147	-2.83	-0.94	63.2	-0.61	-0.80	-45.96	3.73	0.52
25-B-3	-87	-3.64	-0.24	69.3	-0.76	-0.95	-8.90	3.56	0.34
25-C-1	-377	0.45	-0.22	99.9	-0.93	-0.23	126.00	-6.11	-9.98
25-C-2	-65	-2.76	-0.74	71.7	1.00	1.33	-32.06	2.47	0.33
25-C-3	-125.5	-2.34	-0.80	70.4	-0.36	-0.50	-10.07	2.84	0.08

Table 7. Normalized percent change results for each parameter and test.

Test ID	%Δ Volume	%Δ DO	%Δ pH	%Δ COD	%Δ Total P	%Δ Ortho PO_4^{3-}	%Δ TSS	%Δ TN	%Δ TON
5-B-1	-73.75	-50.34	-4.90	530	-51.03	-63.43	350	-84.55	-96.92
5-B-2	-48.75	-20.64	-15.90	6640	-28.91	-58.73	-64.52	90.62	230.30
5-B-3	-23.75	-35.99	25.82	1167	33.48	-1.92	54.48	80.87	1470000
5-C-1	-63.75	-21.83	5.55	6070	-27.67	-46.98	-	-57.89	-100.00
5-C-2	-33.25	-1.22	-13.43	7610	7.09	-20.33	-	197.98	1011.11
5-C-3	-12.13	-30.46	-7.61	1997	-31.84	-34.11	-55.58	31.37	0.00
10-B-1	-68.27	-22.26	-16.08	7570	-56.83	-56.39	-36.00	79.28	0.00
10-B-2	-41.92	-19.00	-12.79	6710	-37.96	-52.21	-87.94	98.28	-1.25
10-B-3	-21.15	-49.13	-11.71	6430	-46.92	-28.23	-83.39	86.84	100000
10-C-1	-59.04	-8.48	-3.82	2492	2.07	-25.00	440.00	243.97	163.83
10-C-2	-28.85	-20.18	-13.15	8460	-10.64	-37.23	-90.10	199.43	140.74
10-C-3	-3.94	-27.30	-12.50	6690	-25.18	-27.47	-77.82	36.68	0.00
25-B-1	-66.41	-7.66	-5.82	6310	-40.39	-35.40	-	-57.57	-89.84
25-B-2	-22.97	-32.34	-12.05	6320	-45.86	-61.07	-82.13	119.94	520000
25-B-3	-13.59	-40.67	-2.98	6930	-51.01	-72.12	-49.73	156.83	340000
25-C-1	-58.91	5.42	-2.64	9990	-44.71	-21.30	5040.00	-50.37	-87.77
25-C-2	-10.16	-29.36	-8.47	7170	53.76	114.84	-64.05	79.94	330000

Table 8. Results for average percent change for each parameter, and results of the Wilcoxon Signed Rank Test. Note: Grey highlight indicates the null hypothesis is rejected.

	Average change (%)		Wilcoxon Signed Ranks Test
Parameter	**Bioretention**	**Control**	**p value**
Volume	-42.28	-32.18	0.011
DO	-30.89	-17.63	0.015
pH	-6.27	-7.15	0.594
COD	5400.80	6391.02	0.008
Total P	-36.16	-11.55	0.110
Ortho PO_4^{3-}	-47.72	-15.03	0.038
TSS	-49.89	14.27	0.499
TN	63.39	86.37	0.260
TON	2.70E+05	4.57E+04	0.859

5.2 Water Quality Results

5.2.1 Biochemical Oxygen Demand

Three water samples were analyzed by Bureau Veritas Laboratory for BOD_5 analysis (one influent sample and two effluent); all results were reported under the detection limit of 2.0 mg/L.

5.2.2 Field Parameters

In all bioretention samples, and all but one control sample the DO was reduced between the influent and effluent water. For the bioretention cells pollutant removal efficiency results ranged from -7.67 to -50.34 %, with an average of -30.89 %. In the control cells the results ranged from +5.42 to -59.03 %, with an overall average of -17.62. The p value for the Wilcoxon Signed Ranks Test is 0.011 (Table 6), therefore the null hypothesis is rejected. Results are displayed graphically in Figure 5. In general, both the bioretention and control cells reduced the DO, however the statistical evidence suggests that the bioretention cells have a higher pollutant removal efficiency for DO, significantly more than the control cells.

The pH was generally reduced from the influent to effluent water in the bioretention cells, only one sample had a positive pollutant removal efficiency. Results range from +25.82 to -16.08 % and the average was -6.27 %. Similarly, the control cells had one positive result with a range from +5.55 % to -13.42 %, and an average of -7.15 % (Figure 6). The p value for these pairs was 0.594 (Table 6), suggesting the null hypothesis cannot be rejected and there is not significant difference between the paired datasets.

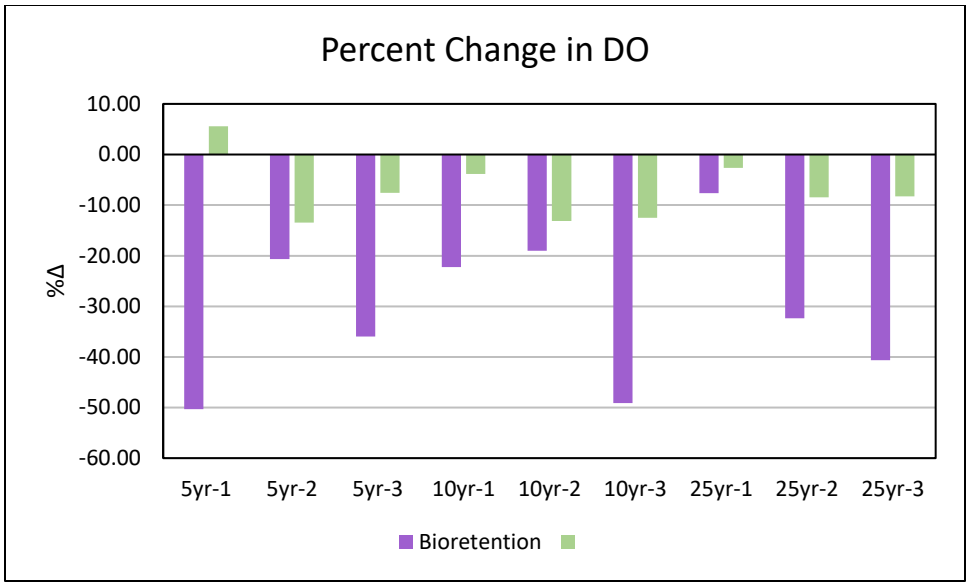

Figure 5. Percent difference for Dissolved Oxygen, in Bioretention and Control cells.

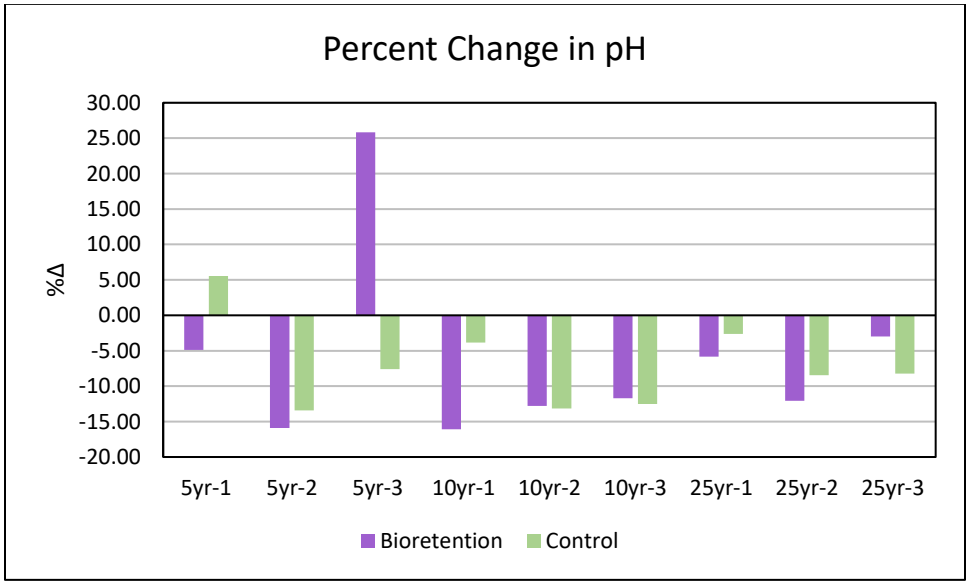

Figure 6. Percent difference for pH, in Bioretention and Control cells.

5.2.3 Chemical Oxygen Demand

COD showed an increase in all samples tested during this study. The bioretention and control cells had pollutant removal efficiency ranges of +530 to +7570 %, and +1997 to +9990 %, respectively. The average increase for the bioretention cells was +5400 %, and for the control cells +6391 %. The p value for COD was 0.008 (Table 6), suggesting that the bioretention

cells had a significantly lower pollutant removal efficiency for COD than the control cells. Data is displayed in Figure 7.

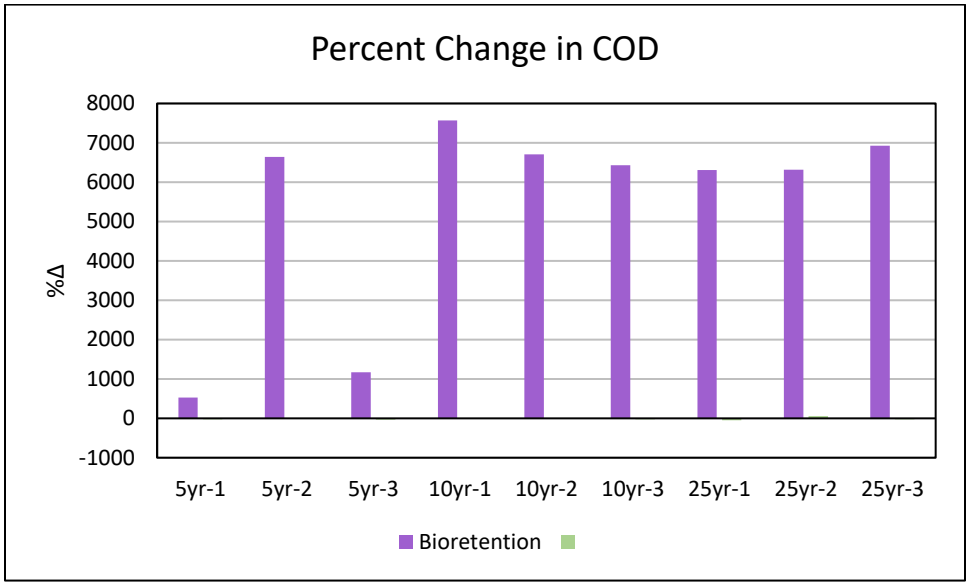

Figure 7. Percent difference for Chemical Oxygen Demand, in Bioretention and Control cells.

5.2.4 Total Phosphorus

In the bioretention cells, total phosphorus was removed in all but one sample, Figure 8 shows the data for total phosphorus. The pollutant removal efficiency ranges from +33.48 to -56.83 %, and the average was -36.15 %. The control cells had similar results; however three samples showed an increase in total phosphorus. The pollutant removal efficiency range for the control cells was +53.76 to -44.71 %, and the average was -11.55 %. The p value for this pair is 0.110 (Table 6) indicating the null hypothesis can be accepted, and there is no significant difference between the two data sets.

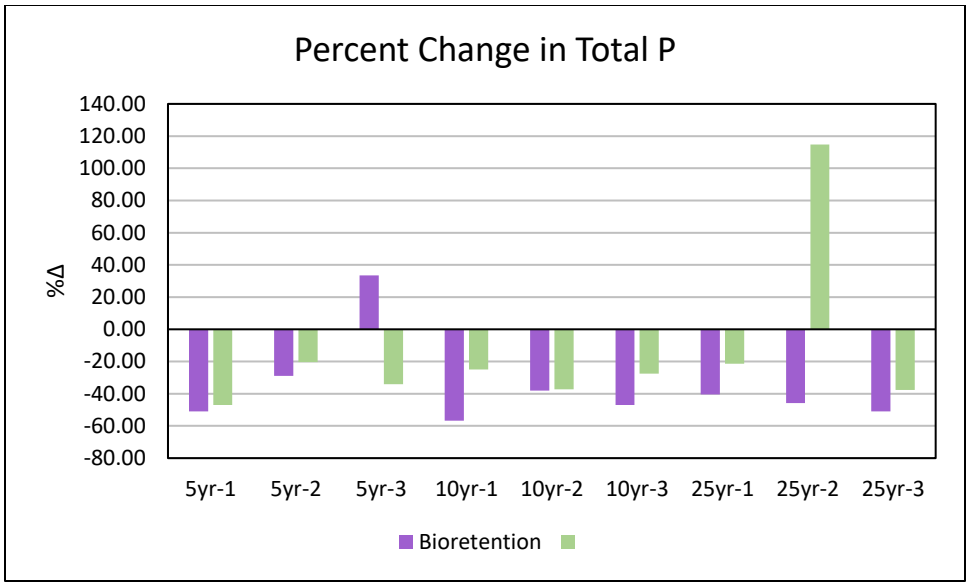

Figure 8. Percent difference for Total phosphorus, in Bioretention and Control cells.

5.2.5 Orthophosphate

The concentration of orthophosphate was reduced in all samples of this study except for one data point in the control cells. The pollutant removal efficiency in the bioretention cells ranges from -1.92 to -56.83 % and averages at -47.72 %. For the control cells the range was +114.84 to -46.98 %, and the average was -15.03 % (Figure 9). The p value for orthophosphate is 0.038 (table 6), indicating the null hypothesis is rejected and the pollutant removal efficiency for bioretention cells is significantly better than the control cells for removing orthophosphate from the water.

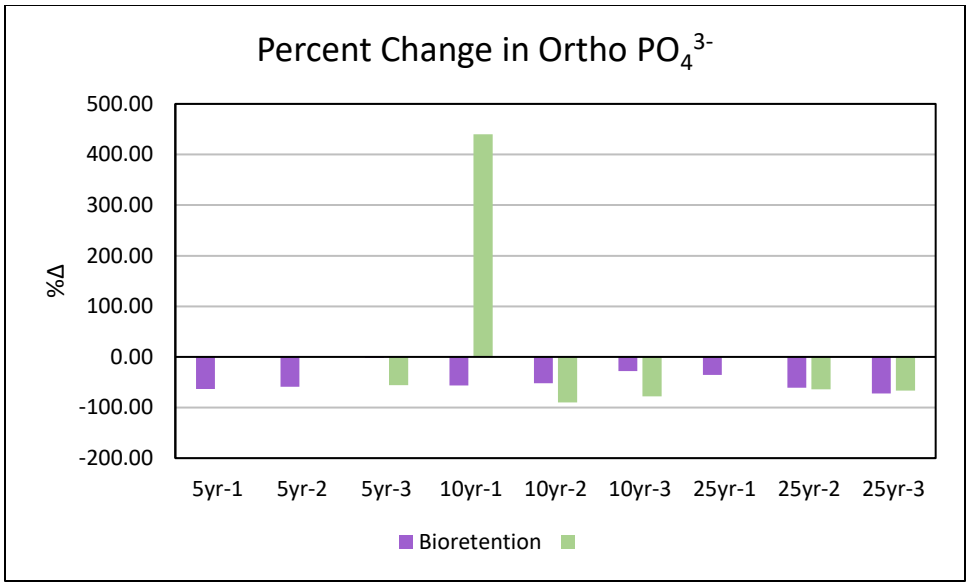

Figure 9. Percent difference for Orthophosphate, in Bioretention and Control cells.

5.2.6 Total Suspended Solids

TSS results varied greatly across the samples in both datasets. For the bioretention cells the pollutant removal efficiency for TSS ranged from +350 to -87.94 %, with an average at -49.89 %. In the control cells the range was +440 to -90.10 %, with the average at +14.27 % (Figure 10). It should be noted that one outlier was removed from the control data for this analysis, which changes the control average to -70.87 %. The p value for TSS is 0.499 (Table 6), the null hypothesis cannot be rejected therefore there is no statistically significant difference between the two datasets.

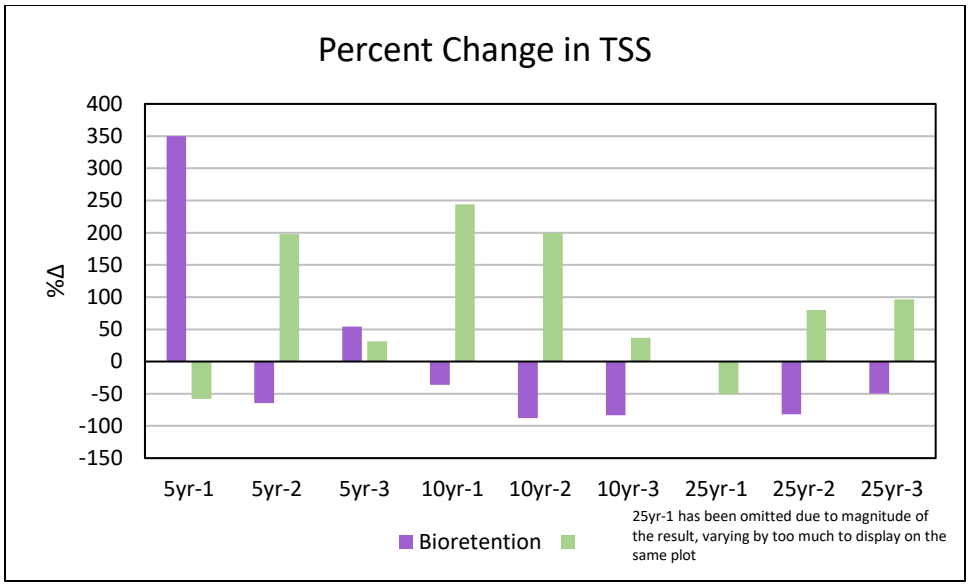

Figure 10. Percent difference over time for Total Suspended Solids, in Bioretention and Control cells.

5.2.7 Total Nitrogen

In all tests except one 5-year and one 25-year event (in both the bioretention and control), nitrogen was leached into the effluent water. In the bioretention cells percent change ranged from -84 – +156 %, in the control it ranged from -58 – +244 % (Figure 11). On average the bioretention and control cells leached TN 63 %, and 86 %, respectively. The p value for the TN tests was 0.260 (Table 6), indicating no statistical significance between the bioretention and control pair.

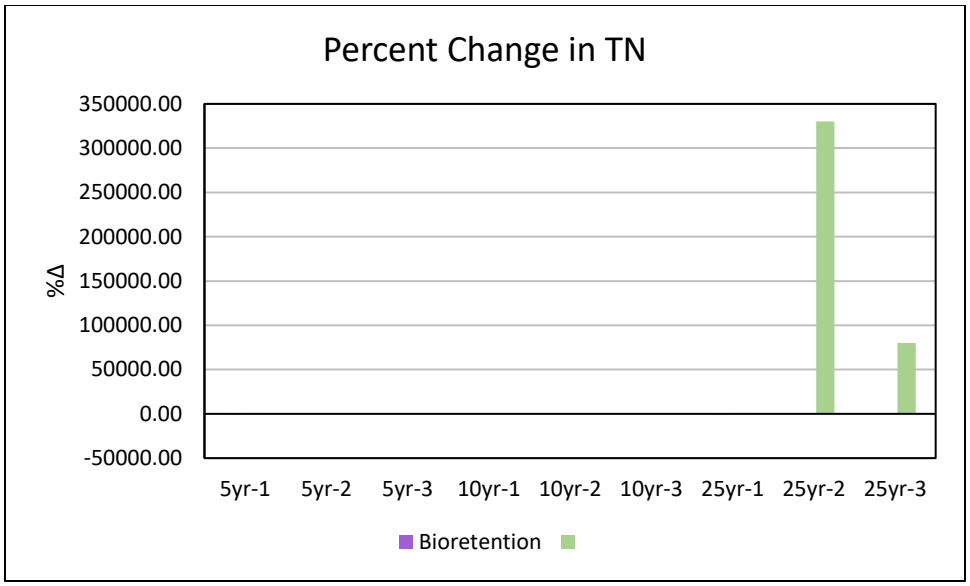

Figure 11. Percent difference for Total Nitrogen, in Bioretention and Control cells.

5.2.8 Total Organic Nitrogen

Pollutant removal efficiency results for TON varied largely in magnitude and sign, to capture all the results they are displayed on both Figures 12, and 13 (note the magnitude of each scale). In three bioretention and two control tests TON was reduced in the effluent water, leaching occurred in all other tests however, some resulted in no change. For the bioretention cells the percent change ranged from -97 - $+1.47 \times 10^6$ %, and in the control cells the range was -100 - $+3.30 \times 10^5$ %. The average pollutant removal efficiency for the bioretention cells was $+2.70 \times 10^5$ %, and for the control cells $+4.57 \times 10^4$ %. The p value for this pair was 0.859 (Table 6), indicating there is no statistically significant difference in the results of the pair.

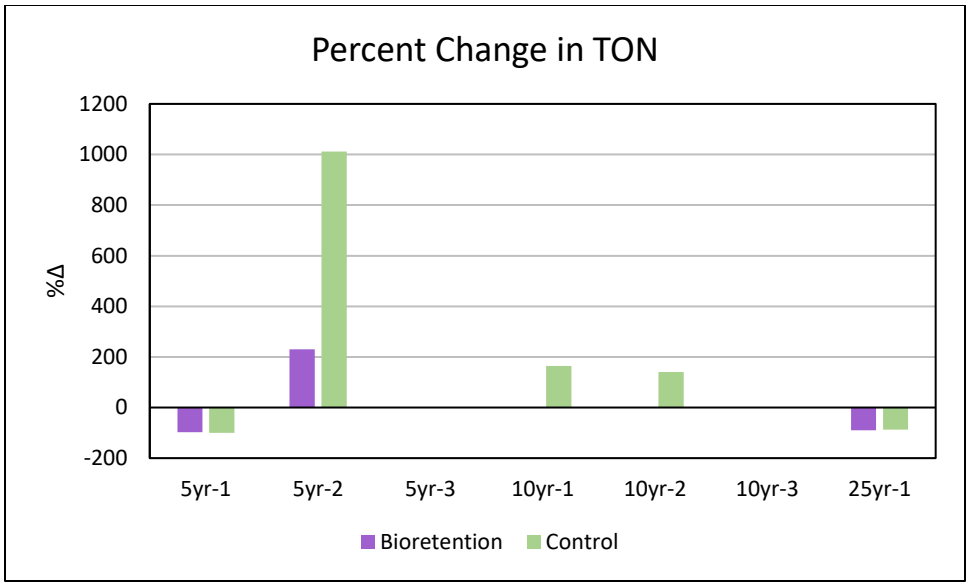

Figure 12. Percent difference for Total Organic Nitrogen, in Bioretention and Control cells. Plot 1 of 2.

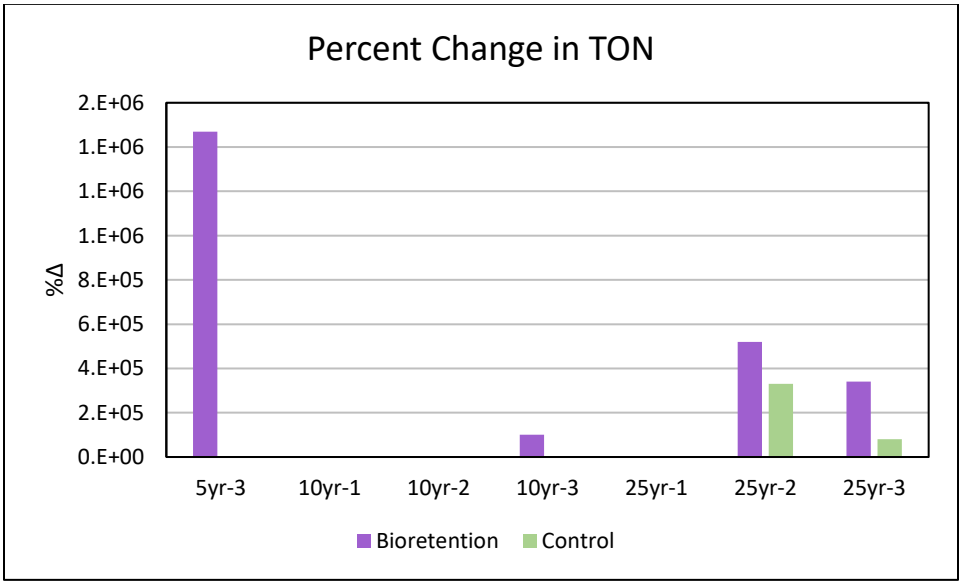

Figure 13. Percent difference for Total Nitrogen, in Bioretention and Control cells. Plot 2 of 2.

5.3 Hydrologic Results

5.3.1 Mass Balance

Every test in this study was successful at water volume retention (Figure 14). The water retention rate for the bioretention cells ranged from -14 – -74 %, and the control cells -4 – -64

%. The average water retention rates were -42, and -32 % for the bioretention and control cells, respectively. The p value for this bioretention and control pair was 0.011, indicating a statistically significant difference between the two. In this case the bioretention cells were significantly better at water volume retention than the control cells.

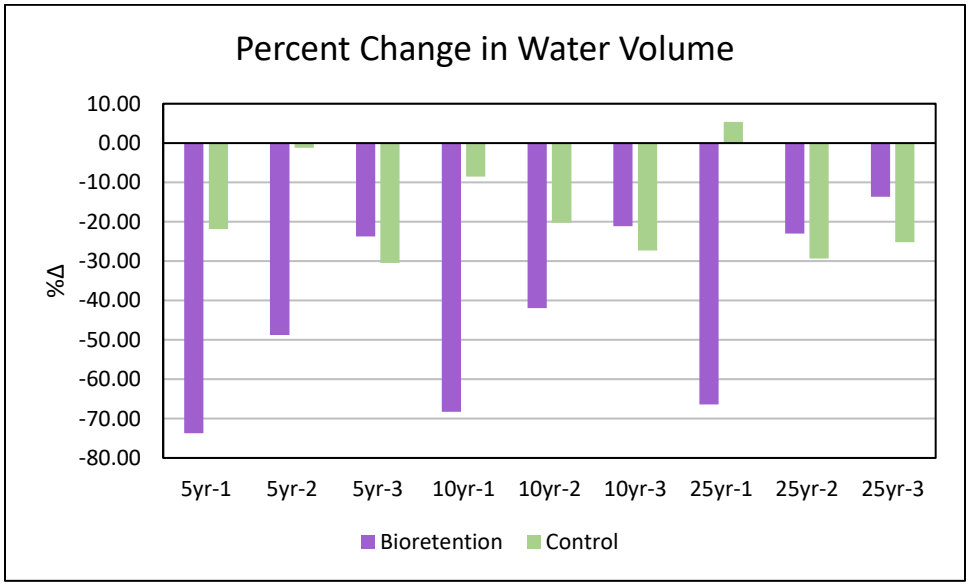

Figure 14. Percent difference for total water volume, in Bioretention and Control cells.

5.3.2 LAI Data

Based on the nature of recording LAI data with an LAI meter, records can be lower than the true value due to the presence of clouds and exact angle of the sun. However, overestimation of LAI with an LAI meter is not possible. With this knowledge, the 5-record moving maximum curve (Figure 15) is considered the most accurate representation of LAI for this study. The maximum recorded LAI value was 3.59 on September 29, 2020. For the reasons described above and based on common literature values of similar deciduous trees at the end of growing season to beginning of senescence (ASCE 1996; Luo et al., 2017), this value can be used as the LAI for the site from the beginning of the study period to its recorded date.

Following the peak LAI, values consistently drop to reach a minimum of 0.64 on October 30, 2021. The period between September 30 and October 29 when LAI was dropping indicates the abscission period, when necrotic leaf material was dropped from the vegetation. Based on LAI and visual observations of chlorophyll degradation described in section 4.3.1, the portion of the study period from August 15 to September 30 took place during plant senescence and the remainder of the study period from September 30 to October 7, took place during senesce and abscission. The plants in the study site entered their winter dormancy by October 30.

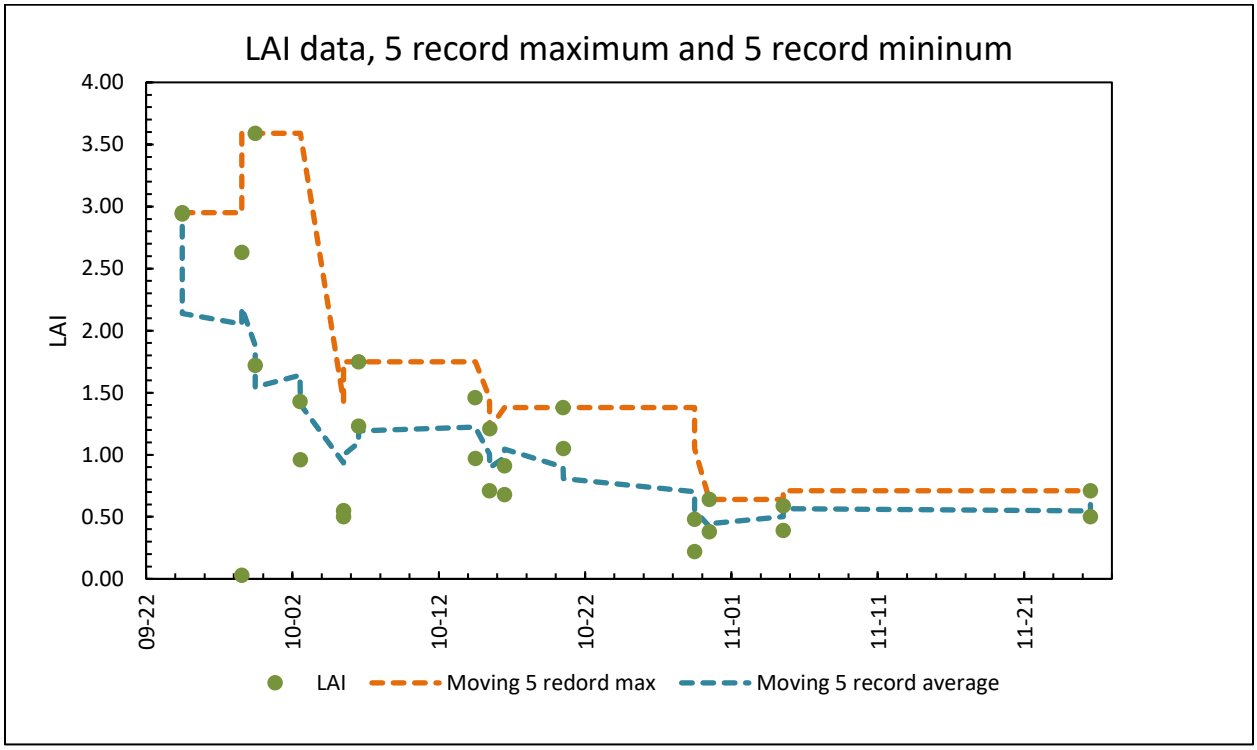

Figure 15. LAI data, 5-record max, and 5-record average are given throughout the study period.

5.3.3 MET Station Data and Water Volume Retention

Windspeed and temperature are the two biggest environmental influences on ET. Weather station data for daily windspeed and temperature throughout the study period are

given in Figures 16 and 17, respectively. Figure 16 shows daily maximum and average windspeed varied from day to day within the study period but remained relatively constant with no major positive or negative trend. Figure 17 shows that daily temperature (maximum, average, and minimum) overall decreases throughout the study period, except for an unusual low on September 12.

Spearman's Rho correlation coefficients between MET station parameters and the water retention rate are given in Table 9, for both the bioretention and control cells.

In the bioretention cells strong positive correlations were found for temperature (all of daily maximum, average and minimum), as well as daily average wind. These pairs had correlations ranging from 0.717 to 0.767. Moderate to weak positive correlations were found for daily maximum wind, maximum PAR, and average PAR, which ranged from 0.017 to 0.433. The remaining parameters (daily maximum humidity, average humidity, and average PAR) resulted in moderate magnitude negative correlations ranging from -0.233 to -0.469. The correlations with daily maximum temperature, average temperature, minimum temperature, and average wind were significant at the 0.05 level. No other correlations for the bioretention cells were statistically significant.

All correlations between water retention rate and the MET station parameters for data in the control cells were weak to moderate. Positive correlations ranging from 0.183 to 0.333 were found for all daily temperature (maximum, average, and minimum), as well as maximum PAR. Negative correlations were found for the remaining parameters; daily maximum wind, average wind, maximum humidity, average humidity, minimum humidity, and average PAR. The

magnitudes of the negative correlations range from -0.083 to -0.483. None of the Spearman's Rho correlation coefficients between the water retention rate and MET station parameters were statistically significant.

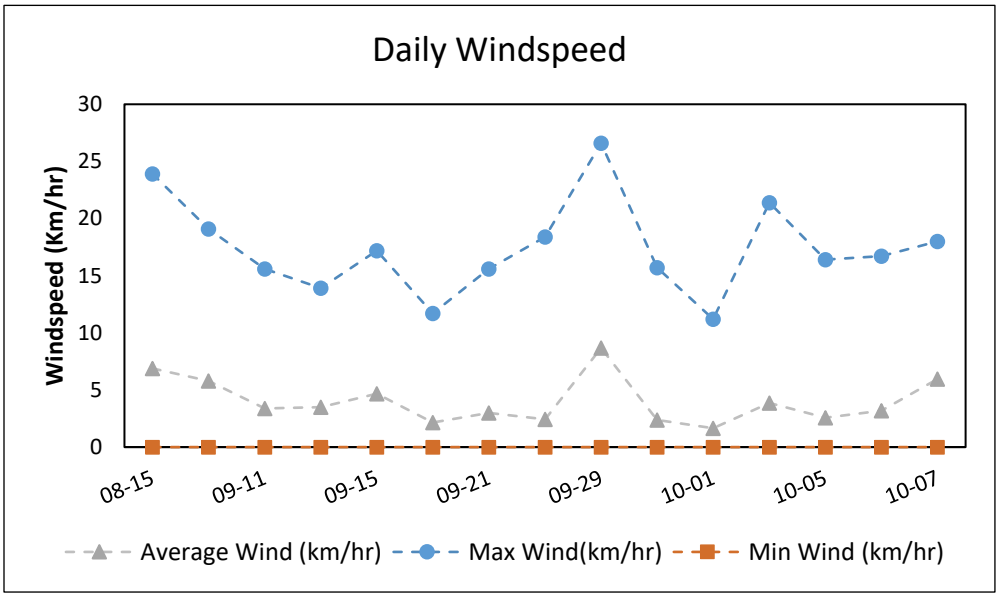

Figure 16. Daily maximum, average, and minimum windspeed are given throughout the study period, as recorded by the MET station on the field site.

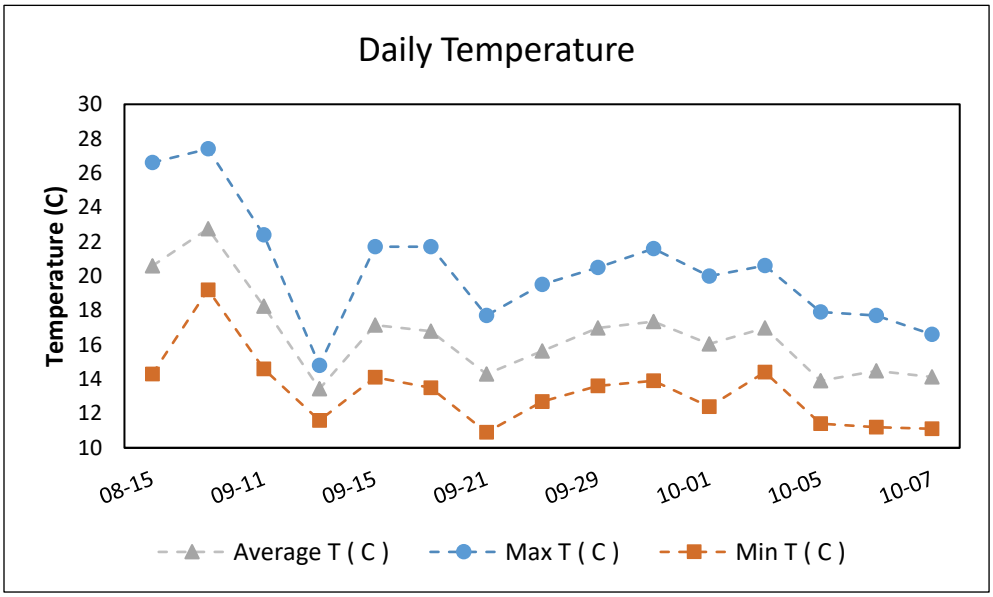

Figure 17. Daily maximum, average, and minimum temperature are given throughout the study period, as recorded by the MET station on the field site.

Table 9. Correlation coefficients between water retention rate, ET and each MET station parameter.

Correlation with %Δ Volume Bioretention		***Correlation with %Δ Volume Control***	
ET_C (mm/day)	0.717*	ET_0 (mm/day)	0.184
Max T (°C)	0.753*	Max T (°C)	0.218
Average T (°C)	0.717*	Average T (°C)	0.200
Min T (°C)	0.733*	Min T (°C)	0.183
Max Wind(km/hr)	0.385	Max Wind(km/hr)	-0.483
Average Wind (km/hr)	0.767*	Average Wind (km/hr)	-0.233
Min Wind (km/hr)	-	Min Wind (km/hr)	-
Max Humidity (%)	-0.233	Max Humidity (%)	-0.154
Average Humidity (%)	-0.283	Average Humidity (%)	-0.083
Min Humidity (%)	-0.469	Min Humidity (%)	-0.350
Max PAR (W/m^2)	0.017	Max PAR (W/m^2)	0.333
Average PAR (W/m^2)	0.433	Average PAR (W/m^2)	-0.067
Min PAR (W/m^2)	-	Min PAR (W/m^2)	-

* Significance at the 0.05 level

- indicates the minimum value was 0

5.3.4 Daily ET and Water Volume Retention

Daily reference ET (ET_0) was converted to daily crop ET (ET_c) for test days on the vegetated bioretention cells,using a crop coefficient (K_c). ET_0, K_c, and ET_c are given by date in Table 10. On all dates except for the last test, the ET_c is higher than the ET_0. ET_0 values range from 1.20 - 4.70 mm/day, whereas ET_c values range from 0.89 – 24.69 mm/day.

Table 10. Daily reference ET, LAI, crop coefficient, and resulting crop ET for each test day in the study period.

Date	**ET_0 (mm/day)**	**LAI Max**	**K_c**	**ET_c (mm/day)**
15-Aug	4.70	3.59	5.25	24.69
17-Aug	4.70	-	-	-
11-Sep	2.70	3.59	5.25	14.18
12-Sep	1.20	-	-	-
15-Sep	2.20	3.59	5.25	11.56
17-Sep	1.40	3.59	5.25	7.35
21-Sep	1.60	3.59	5.25	8.40
22-Sep	2.00	3.59	5.25	10.51
29-Sep	2.50	-	-	-
30-Sep	1.80	3.59	5.25	9.45

01-Oct	1.50	3.59	5.25	7.88
02-Oct	1.80	-	-	-
05-Oct	1.20	1.75	0.74	0.89
06-Oct	1.40	-	-	-
07-Oct	1.20	-	-	-

Similar to the MET station data, a Spearman's Rho correlation coefficient was calculated for the relationship between daily ET and the water retention rate, in both the bioretention and control cells. This relationship is also displayed in Figure 18, with daily ET throughout the study period and the water retention rate for each test. Both test groups resulted in a positive correlation; the bioretention cells at 0.717, and the control cells at 0.184 (Table 9). The correlation between ET and water retention rate for the bioretention dataset is significant at the 0.05 level, conversely, the same correlation in the control dataset is not statistically significant.

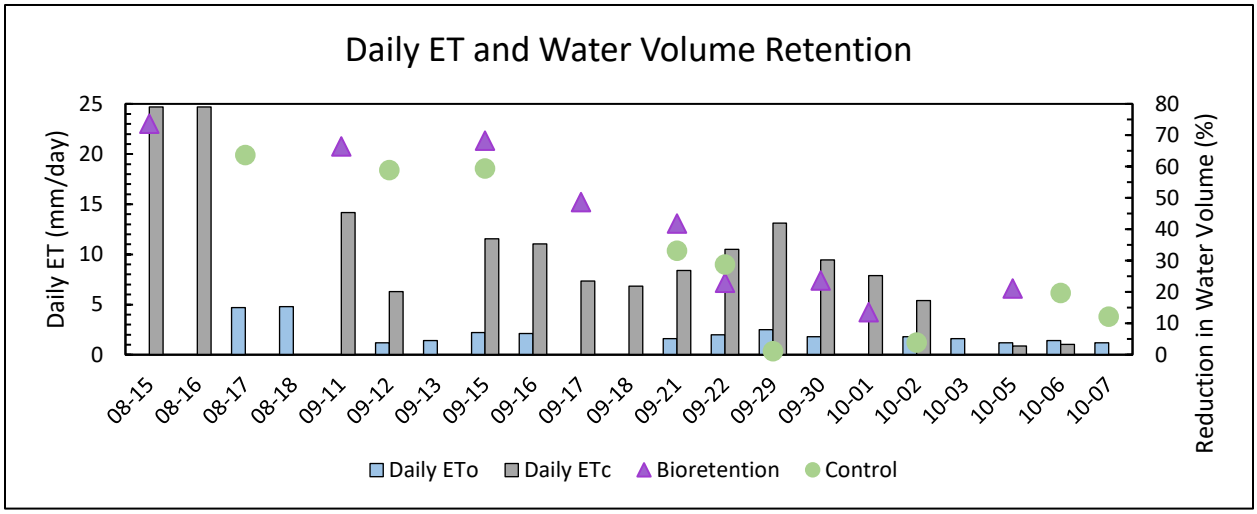

Figure 18. Daily ET_0 is provided by the blue bars and ET_c by the grey bars with scale on the left vertical axis, water retention rate is given by the points (purple triangles corresponding to bioretention and green squares corresponding to control cells) with scale on the right.

5.3.5 Soil Moisture Data

Field capacity (FC) and Antecedent Moisture Content (AMC) are indicated in Figure 19, which shows soil moisture data at 20 cm depth (within the rooting zone) for both the vegetated bioretention cell and the control cell. FC for the vegetated and control cells were determined to be 0.28, and 0.18 m^3/m^3, respectively. AMC in the dry, pretested soil was determined to be 0.14 and 0.08 m^3/m^3 , for the vegetated and control cells. Both the FC and AMC are higher in the vegetated cells, likely attributed to the rooting zone holding more water in the vegetated cells.

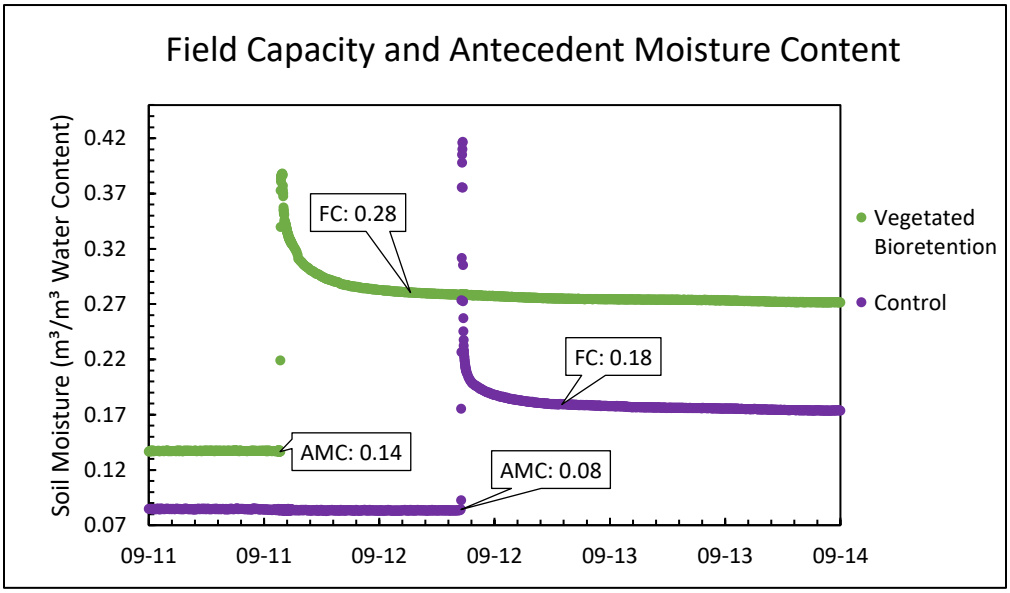

Figure 19. Determination of field capacity (FC) and antecedent moisture content (AMC) at 20 cm depth in the test cells.

The soil moisture (SM) data is presented below in Figures 20 and 21. The data was split between two plots for ease of viewing, and period of time between September 23rd, 2020 and September 28th, 2020, was removed as this was a period of natural rainfall and no tests could be conducted. The data from tests on August 15th and 16th recorded no signal, this is attributed

to an error in the sensors. Plots for this time period have been omitted below but are provided in Appendix D. Both plots display the same trend where the soil moisture spikes during a test then is subject to rapid gravity drainage back to the cell's field capacity (where the curve flattens out), a visual display of each phase is given Figure 22. In both the control and the bioretention cells, the shallower SM probes recorded a lower water content than the deeper probes. The high permeability of soils resulting in little to no retention of water within the soils, suggests that the portion of ET attributed to evaporation from soil at this test site is negligible.

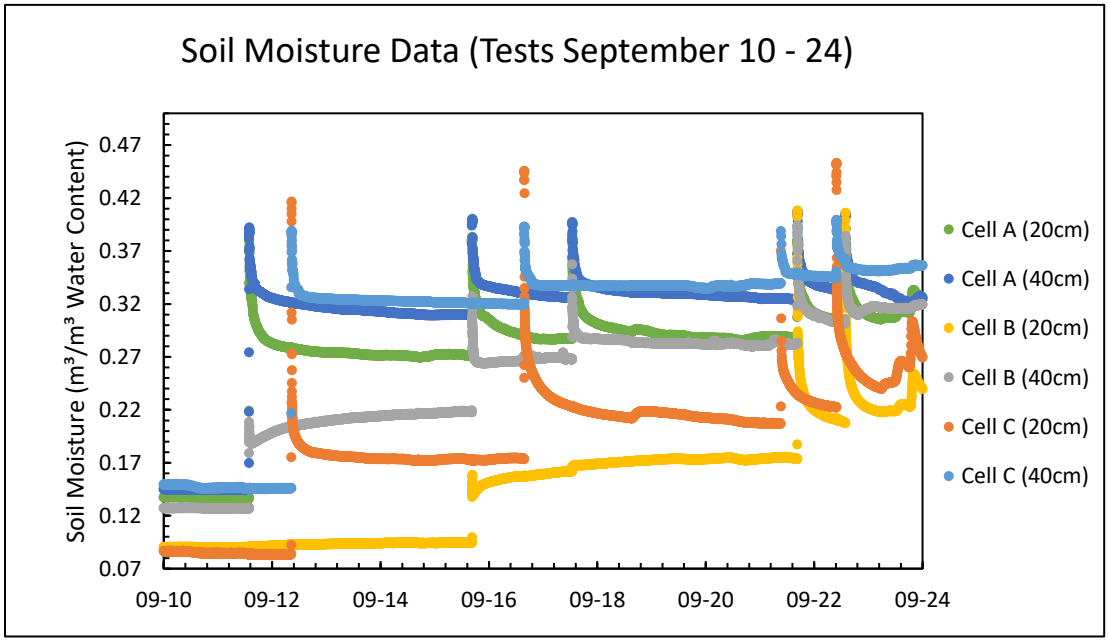

Figure 20. Soil moisture data from September 10th to September 24th. Location and depths of SM probes is indicated in the legend; cell configuration is provided in figure 2.

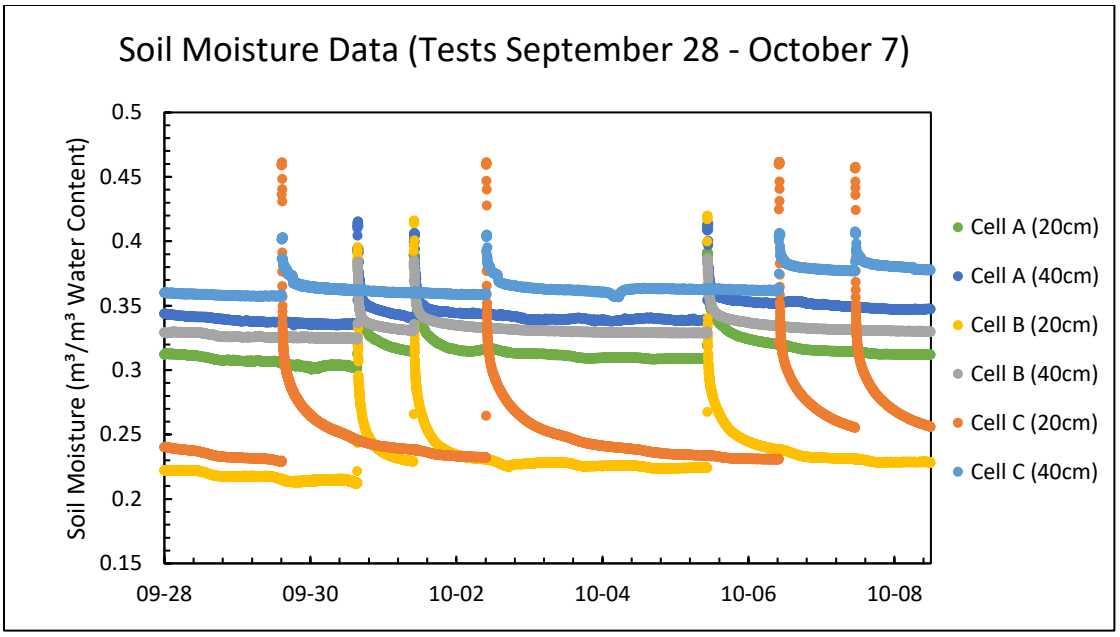

Figure 21. Soil moisture data from September 28th to October 8th. Location and depths of SM probes is indicated in the legend; cell configuration is provided in figure 2.

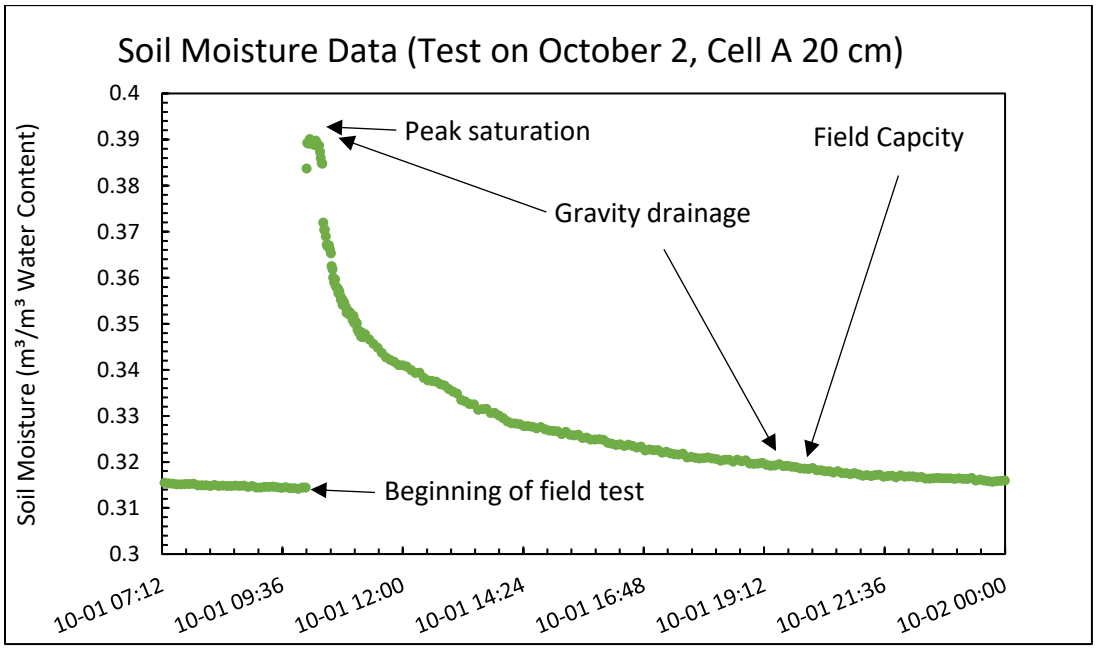

Figure 22. Example of timeline for field test on soil moisture. Note: Arrows are meant to provide a visualization of each mechanisim and stage of water application and removal not exact points.

6.0 Discussion

6.1 Water Quality Performance and Role of Vegetation

In general, both the bioretention cells and control cells reduced pH, DO, total phosphorus, orthophosphate and total suspended solids.

pH in the influent water generally ranged from neutral to basic. A minor acidification process took place in the soil of the cells, in all but two tests the pH was reduced by 0.24 to 1.23 pH units. This process was consistent across all tests and given the results of the statistical analysis, it is likely a result of the soil - water interaction, or atmosphere - water interaction and not a function of the bioretention system or influenced by the vegetation.

In all but one test the DO was reduced from the influent to the effluent water. The bioretention cells overall reduced the DO approximately two times more than the control cells. In this case the statistical analysis indicated the results were statistically different. Because deoxygenation took place in both systems there is likely some role of the soils in the process. However, the bioretention cells caused significantly more deoxygenation than the control cells which is likely a cause of the decaying plant material (due to annual senescence) using up oxygen.

With the exception of a few outliers, both total phosphorous and orthophosphate were consistently removed by both the bioretention and control cells. In the case of both phosphorous forms, the bioretention cells reduced the effluent concentration by approximately three more times than the control cells. Although on average the bioretention cells were more effective at removing total phosphorous from the water, the results were not statistically

significant. Therefore, no conclusion can be made on the difference between the bioretention and cells and the control cells' ability to remove total phosphorous. However, the results for orthophosphate were statistically significant, indicating that the bioretention cells were more effective at removing orthophosphate from the water than the control cells. The control cells did remove approximately one third the amount of orthophosphate than the control cells, indicating that some of the removal was likely from an organic process in the soil as orthophosphate is the form of phosphorous most readily used by organic organisms. The difference in the two systems may be attributed to the vegetation in the bioretention cells, and uptake of the phosphate species by plants for nutrients.

In the majority of tests TSS was reduced in the effluent water. The bioretention cells removed much more TSS with an average -49.89 %. The control cells averaged an addition of 14.27 %, however, that average is largely influenced by one event. If this event is excluded from the calculation, the average for the control cells is -70.87 %. With the exclusion of outliers in the data, both the bioretention and control cells are effective at removing TSS loads from effluent water. The p value indicates no statistical difference between the bioretention and control cells. This is to be expected as the vegetation likely plays very little role in TSS removal. The soil media capturing particles is much more likely the mechanism of particle removal. Four TSS tests had lab errors and were not included in this analysis.

Overall COD, TN, and TON were all of higher concentration in the effluent water when compared to the influent water.

The concentration of COD was greatly increased in every test of this study. The bioretention cells increased COD an average of 5400 % and the control cells 6391 %. These results mean large concentrations of chemically oxidizable organics were leached into the effluent water from the soil. Although the average results of the bioretention and control cells are similar, the p value was small enough to reject the null hypothesis, therefore results between the bioretention and control cells are significantly different. It can be said that the vegetation played a role in reducing the COD pollution. Conversely, all BOD_5 samples sent for analysis were reported below the lab's detection limit. BOD represents biochemically oxidizable organics and generally for any given water type, a BOD:COD ratio is consistent. When COD is much larger than BOD, it may act as an indicator of industrial waste or high toxicity. The large presence of COD, and lack of BOD in the effluent water is a unique result and unexpected for a controlled study site.

Overall, TN and TON were both leached into the effluent water. In two bioretention tests and two control tests, total nitrogen was decreased from the influent to the effluent water. However, on average the bioretention cells increased the total nitrogen by +63 % and the control cells by +86 %. The results for total organic nitrogen were highly variable, in both sign and magnitude. Due to some large values the averages were an increase of $+2.7x10^5$ %, and $+4.57x10^4$ %, for the bioretention and control cells respectively. Although on average the results show leaching of the both TN and TON, the results are widely variable and no conclusion can be made. The TON results in the bioretention cells is an order of magnitude larger than the control cells, which could be attributed to decaying plant matter. However, the results for both

nitrogen species between the bioretention and control cells were not statistically different, therefore no comment can be made on the role of vegetation.

6.2 Hydrologic Performance and Role of Vegetation

All tests in this study were successful in reducing the effluent water volume. The average water retention rate for the bioretention cells was 42 %, and for the control cells 32 %. The bioretention cells were statistically more effective at reducing the effluent water volume. The mechanism of water removal is evapotranspiration; evaporation directly from the soil, and transpiration through the vegetation. Given that the control cells were able to reduce the effluent volume; it could be suggested that evaporation played a large role in the water volume retention. However, the presence of plants, and ability of vegetation to uptake, store, and transpire water was able to increase the effectiveness by 10 %, and the soil moisture data displayed a rapid to drop to field capacity due to gravity drainage which would conversely suggest little contribution to ET by evaporation alone.

When the correlations between water volume retention and both ET and MET station parameters are compared between the bioretention and control cells, the signs are generally the same across both datasets. Three MET station parameters do not follow this pattern; maximum wind, average wind, and average PAR. In the case of these three parameters the result for the bioretention data is positive but the result for the control cells is a negative correlation. In cases where the signs between the datasets match, the bioretention data correlations tend to have a much larger magnitude than the control dataset in both the positive and negative directions. In the bioretention dataset strong correlations were all positive and

corresponded to ET, all three measures of temperature and average wind. Conversely, in the control cells no strong correlations are reported. This suggests that a positive relationship does in fact exist between the magnitude of ET and the presence of vegetation in a bioretention system and that higher temperatures and wind speeds may enhance the removal of water by vegetation. Interestingly, only five of the twenty-two calculated correlation coefficients were statistically significant, and all of these were in the bioretention dataset. The lack of statistical significance in the results is likely due to the small sample size of this study, but results do point to a conclusion that the presence of vegetation plays a large role in the removal of water through ET in bioretention systems when compared to a grass control.

7.0 Conclusions and Recommendations

7.1 Study Conclusions

The objectives of this study were to:

1. Determine the ability of Bioretention cells to remove nutrient pollutants and TSS during plant senescence and abscission;
2. Determine the hydrologic ability of bioretention cells to reduce peak runoff loads through evapotranspiration during plant senescence and abscission, and;
3. Investigate the role of vegetation in both the water quality and hydrologic performance of bioretention cells.

A total of 18 individual, full-scale bioretention rainfall runoff simulations were successfully conducted at the field site located at University of Victoria, during the plant Senescence period in late 2020. Lab analytical testing and statistical analysis on samples collected during the study can provide the following insights:

1. Bioretention systems perform pollutant removal from runoff water of TSS, and Phosphorous species, but conversely leaching Nitrogen species during the plant senescence period.
2. Bioretention systems maintain water retention during peak loads during the plant senesce period, through the mechanisms of evaporation and transpiration.
3. The presence of treed vegetation plays a significant role in the removal of Orthophosphate and water retention in bioretention systems when compared to a

grass control. Additionally, allowing plant matter to decay within the cells may reduce dissolved oxygen levels in the effluent water.

7.2 Recommendations for Future Research

Future work in this field should consider an increase in temporal scale. Conducting the same or similar tests for a longer period of time, over multiple seasons, vegetation growth states, and years could provide much more insight into the abilities of bioretention systems. Obtaining a larger dataset would allow for more complex analyses to be run on the data, and would allow for testing and rejection of true outliers. Data sets spanning the entirety of a plant growth cycle at one site, would allow for comparison of concentrations of nutrient and organic pollutants through each phase. Multiyear data would be beneficial in three ways (1) to study if results change due to climatic changes from year to year, (2) to determine if any pollutant removal or leaching becomes more extreme over time, if the systems become saturated with a given pollutant, and (3) confirm or dispute results of this study with a larger dataset for more in-depth statistical analysis.

In the case of this site, further analysis into the soil water interactions would be extremely beneficial. Many of the results could not be discerned between the bioretention cells and the control cells, indicating a large role of the soil in the water chemistry changes. In addition, the results for COD and DO, indicated a large presence of oxidizers and biodegradation resistant organics. A study into the microorganism profile of the soil would be a key to further understanding the water quality results of this work. Perhaps through an environmental DNA study of the soil.

References

Aryal, R., Vigneswaran, S., Kandasamy, J. et al. (2010) Urban stormwater quality and treatment. Korean J. Chem. Eng. 27, 1343–1359.

ASCE (1996) Chapter 4: Evaporation and Transpiration. Hydrology Handbook, 2nd ed. American Society of Civil Engineers.

Barlow, D., Burrill, G., and Nolfi, J., 1977. Research report on developing a community level natural resource inventory system: Center for Studies in Food Self-Sufficiency.

Barrett, M.E., Limouzin, M., Lawler, D.F. (2013) Effects of Media and Plant Selection on Biofiltration Performance. Journal of Environmental Engineering, 139: 462-470.

Barron, N.J., Hatt, B., Jung, J., Chen, Y., Deletic, A. (2020) Seasonal operation of dual-mode biofilters: The influence of plant species on stormwater and greywater treatment. Science of The Total Environment, 715: 136680.

Berland, A., Shiflett, S.A., Shuster, W.D., Garmestani, A.S., Goddard, H.C., Herrmann, D.L., Hopton, M.E. (2017) The role of trees in urban stormwater management. Landscape and Urban Planning, 162: 167-177.

Bonneau, J., Fletcher, T. D., Costelloe, J. F., et al. (2020) The hydrologic, water quality and flow regime performance of a bioretention basin in Melbourne, Australia. Urban Water Journal. 17(4), 303 – 314.

Campbell, G.S. (n.d.) Plant available water: How do I determine field capacity and permeant wilting point? METER Group, accessed December 2021. https://www.metergroup.com/en/meter-environment/measurement-insights/plant-available-water-determine-field-capacity-permanent-wilting-point

CRD, (2019) Core Area Stormwater Quality Program: 2018 Report. Prepared by Stormwater Quality Program.

Dagenais, D., Brisson, J., Fletcher, T.D. (2018) The role of plants in bioretention systems; does the science underpin current guidance? Ecological Engineering, 120: 532-545.

Davis, A. P., Shokouhian, M., Himanshu, S., & Minami, C. (2006). Water quality improvement through bioretention media: Nitrogen and phosphorus removal. Water Environment Research, 78(3), 284-293.

Davis, A. P. (2007). Field performance of bioretention: Water quality. Environmental Engineering Science, 24(8), 1048-1064.

Dunn, A. D. (2010). Siting Green Infrastructure: Legal and Policy Solutions to Alleviate Urban Poverty and Promote Healthy Communities. Boston College Environmental Affairs Law Review, 37.

Eckart, K., McPhee, Z., Bolisetti, T. (2017) Performance and implementation of low impact development - a review. Sci. Total Environ. 607–608, 413–432.

Environment Canada (2019) *Historical Data, VICTORIA UNIVERSITY CS* BRITISH COLUMBIA. https://climate.weather.gc.ca/climate_data/daily_data_e.html?hlyRange=1994-02-01%7C2019-12-18&dlyRange=1992-12-01%7C2019-12-18&mlyRange=1992-01-01%7C2007-02-01&StationID=6812&Prov=BC&urlExtension=_e.html&searchType=stnName&optLim it=yearRange&StartYear=1840&EndYear=2019&selRowPerPage=25&Line=5&searchMethod=contains&Month=12&Day=19&txtStationName=university&timeframe=2&Year=2019.

EPA, U.S., 2000. Low Impact Development (LID) a Literature Review. United States Environmental Protection Agency, pp. 1–35 EPA-841-B-00-005.

FAO (2009) ET_0 Calculator, Food and Agriculture Organization of the United Nations, https://www.fao.org/land-water/databases-and-software/eto-calculator/en/. Accessed November 2021.

FAO (1998) Chapter 2: FAO Penman-Monteith equation. Crop evapotranspiration – Guidelines for computing crop water requirements – FAO Irrigation and drainage paper 56, Food and Agriculture Organization of the United Nations Rome.

FAO (1985) Chapter 2: Soil and Water. Irrigation Water Management: Training Manual No. 1 - Introduction to Irrigation. Food and Agriculture Organization of the United Nations Rome.

Fletcher, T.D., Shuster, W., Hunt, W.F., et al. (2015) SUDS, LID, BMPs, WSUD and more – The evolution and application of terminology surrounding urban drainage, Urban Water Journal, 12:7, 525-542.

Goh, H.W., Lem, K.S., Azizan, N.A., Chang, C.K., Talei, A., Leow, C.S., Zakaria, N.A. (2019) A review of bioretention components and nutrient removal under different climates—future directions for tropics. Environ Sci Pollut Res, 26: 14904–14919

Gulfishan, M., Jahan, A., Bhat, T.A., Sahab, D. (2018) Chapter 16: Plant Senescence and Organ Abscission. In Sarwat, M. & Tuteja, N. (Ed.) Senescence Signalling and Control in Plants. Academic Press.

Hatt, B. E., Fletcher, T. D., & Deletic, A. (2008). Improving stormwater quality through biofiltration: Lessons from field studies. Proceedings of the 11th international conference on urban drainage (pp. 1-10). Edinburgh, UK: ICUD.

Hatt, B. E., Fletcher, T. D., & Deletic, A. (2009). Hydrologic and pollutant removal performance of biofiltration systems at the field scale. Journal of Hydrology, 365(3-4), 310-321.

Hsieh, C. H., & Davis, A. P. (2003). Evaluation of bioretention for treatment of urban storm water runoff. Proceedings of World Water and Environmental Resources Congress 2003 (pp. 141-148). Philadelphia, PA: ASCE.

Hsieh, C. H., & Davis, A. P. (2005a). Evaluation and optimization of bioretention media for treatment of urban storm water runoff. Journal of Environmental Engineering, 131(11), 1521-1531.

Hvitved-Jacobsen, T., Vollertsen, J., Nielsen, A.H., 2010. Urban and highway stormwater pollution: concepts and engineering. Boca Raton, FL : CRC Press/Taylor & Francis.

Jia, Q. & Wang, Y-P. (2021) Relationships between Leaf Area Index and Evapotranspiration and Crop Coefficient of Hilly Apple Orchard in the Loess Plateau. Water, 13: 1957.

Kim, H., Seagren, E. A., & Davis, A. P. (2003). Engineered bioretention for removal of nitrate from stormwater runoff. Water Environment Research, 75(4), 355-367.

LeFevre, G.H., Paus, K.H., Natarajan, P., Gulliver, J.S., Novak, P.J., Hozalski, R.M., 2015. Review of dissolved pollutants in urban storm water and their removal and fate in bioretention cells. J. Environ. Eng. 141 (1).

Leopold, A.C. (1961) Senescence in Plant Development. Science, 134, 3492: 1727-1732.

Li, H., and Davis, A. P. (2009). Water Quality Improvement through Reductions of Pollutant Loads Using Bioretention. Journal of Environmental Engineering, American Society of Civil Engineers (ASCE), 135(8), 567–576.

Li, C., Peng, C., Chiang, P.-C., Cai, Y., Wang, X., Yang, Z., 2019.Mechanisms and applications of green infrastructure practices for stormwater control: a review. J. Hydrol. 568, 626–637.

Liu, J., Sample, D., Bell, C., and Guan, Y. (2014a). Review and Research Needs of Bioretention Used for the Treatment of Urban Stormwater. Water, MDPI AG, 6(4), 1069–1099.

Liu, J., Sample, D. J., Bell, C., and Guan, Y. (2014b). Review and research needs of bioretention used for the treatment of urban stormwater. Water (Switzerland), 6(4), 1069–1099.

Lopez-Ponnada, E.V., Lynn, T.J., Ergas, S.J., Mihelcic, J.R. (2020) Long-term field performance of a conventional and modified bioretention system for removing dissolved nitrogen species in stormwater runoff. Water Research, 170: 115336.

Lucke, T. & Nichols, P.W.B. (2015). The pollution removal and stormwater reduction performance of street-side bioretention basins after ten years in operation. Science of The Total Environment, 536, 784-792.

Lucke, T., Dierkes, C., Boogaard, F. (2017) Investigation into the long-term stormwater pollution removal efficiency of bioretention systems. Water Sci Technol, 8: 2133-2139.

Luo, Z., Guan, H., Zhang, X. (2017) Photosynthetic capacity of senescent leaves for a subtropical broadleaf deciduous tree species Liquidambar formosana Hance. Scientific Reports, 7, 6323.

Minton, G (2005). Stormwater treatment: Biological, chemical and Engineering Principles. Seattle, WA: Resource Planning Associates.

Nocco, M.A., Rouse, S.E., Balster, N.J. (2016) Vegetation type alters water and nitrogen budgets in a controlled, replicated experiment on residential-sized rain gardens planted with prairie, shrub, and turfgrass. Urban Ecosystem, 19, 1665-1691.

Rycewicz-Borecki, M., McLean, J.E., Dupont, R.R. (2017) Nitrogen and Phosphorous mass balance, retention and uptake in six plant species grown in stormwater bioretention microcosms. Ecological Engineering, 99, 409-416.

Shrestha, P., Hurley, S.E., Wemple, B.C. (2018) Effects of different soil media, vegetation, and hydrologic treatments on nutrient and sediment removal in roadside bioretention systems. Ecological Engineering, 112: 116-131.

Skorobogatov, A., He, J., Chu, A., Valeo, C., and van Duin, B. (2020). The impact of media, plants and their interactions on bioretention performance: A review. Science of the Total Environment, Elsevier B.V., 715, 136918

Szota, C., McCarthy, M.J., Sanders, G.J., Farrell, C., Fletcher, T.D., Arndt, S.K., Livesley, S.J. (2018) Tree water-use strategies to improve stormwater retention performance of biofiltration systems. Water Research, 144, 285-295.

Vijayaraghavan, K., Biswal, B.K., Adam, M.G., Soh, S.H., Tsen-Tieng, D.L., Davis, A.P., Chew, S.H., Tan, P.Y., Babovic, V., Balasubramanian, R. (2021) Bioretention systems for stormwater management: Recent advances and future prospects. Journal of Environmental Management. 292, 112766.

Wang, M., Zhang, D., Wang, Z., Zhou, S., Tan, S.K. (2021) Long-term performance of bioretention systems in storm runoff management under climate change and life-cycle condition. Sustainable Cities and Society, 65: 102598.

Winogradoff, D. A. (2002). The bioretention manual. Prince George's County, MD: Programs & Planning Division, Department of Environmental Resources, Prince George's County, MD.

Yang, Y.-Y., Lusk, M.G., 2018. Nutrients in urban stormwater runoff: current state of the science and potential mitigation options. Curr. Pollut. Rep. 4, 112–127.

Zuo, X., Zhang, A.S., Yu, J. (2020) Microbial diversity for the improvement of nitrogen removal in stormwater bioretention cells with three aquatic plants. Chemosphere, 244: 125626.

Appendix A – Site Engineering Drawings

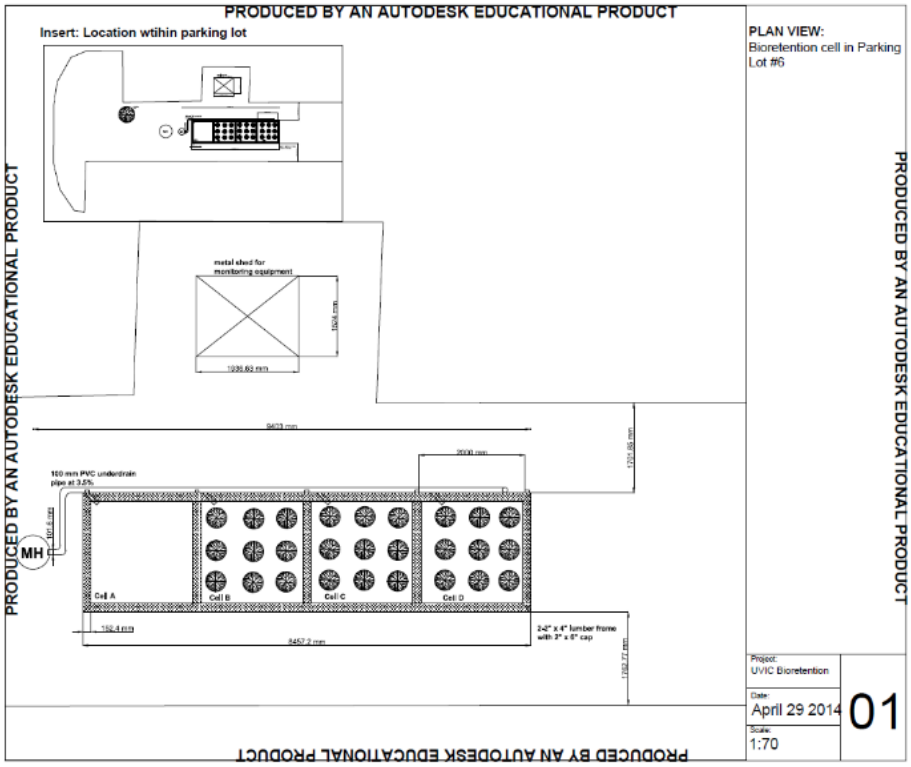

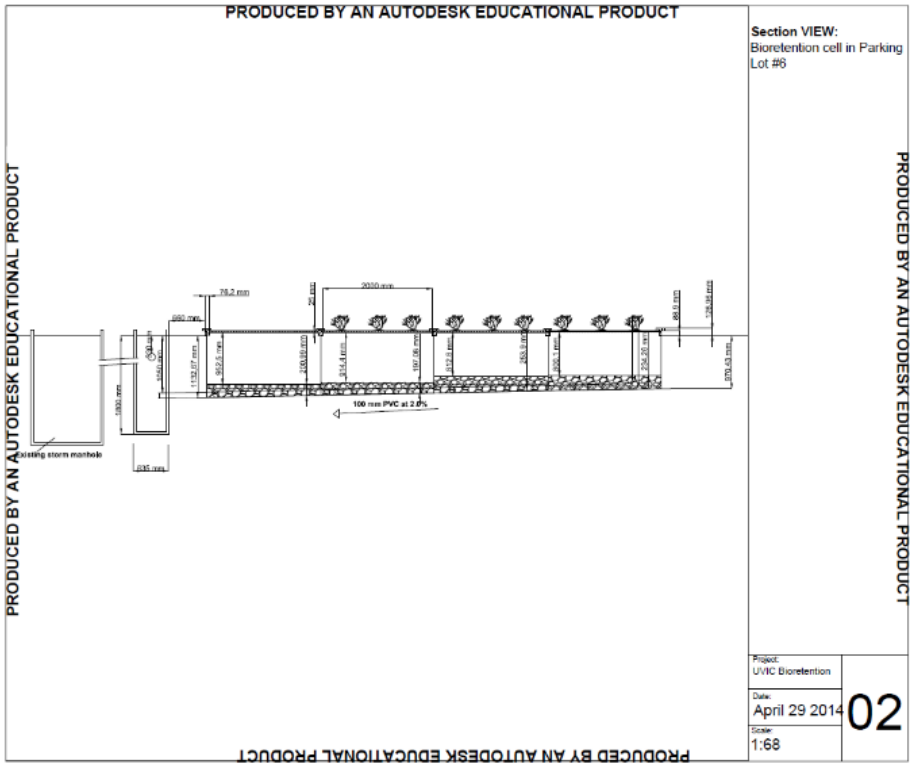

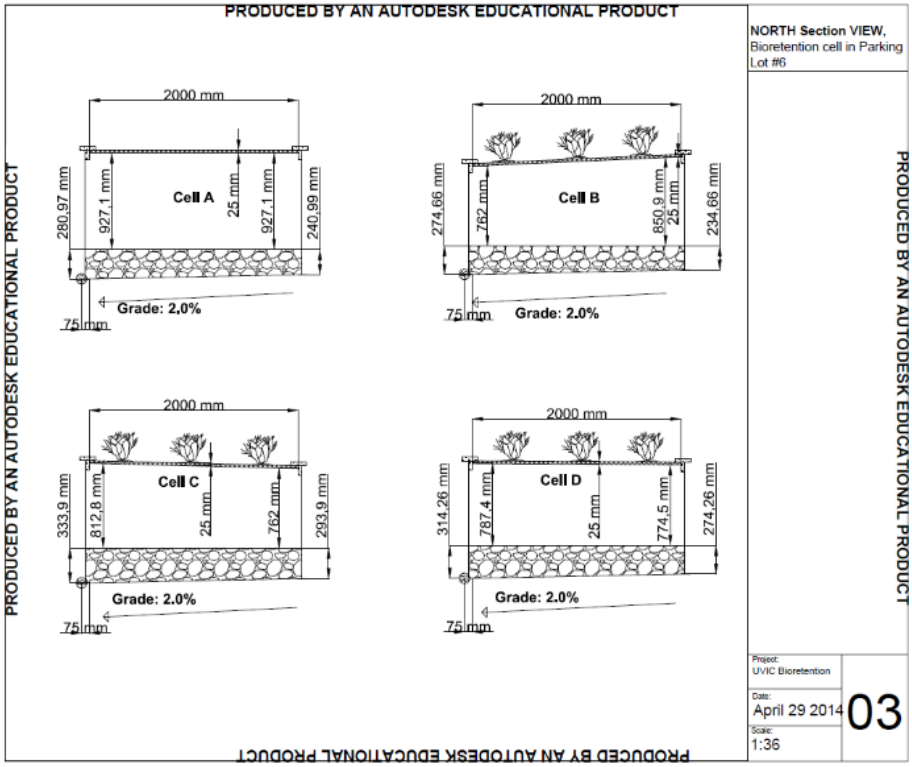
PRODUCED BY AN AUTODESK EDUCATIONAL PRODUCT
NORTH Section VIEW,
Bioretention cell in Parking Lot #6
PRODUCED BY AN AUTODESK EDUCATIONAL PRODUCT
2000 mm
280.97 mm
927.1 mm
Cell A
25 mm
927.1 mm
240.99 mm
Grade: 2.0%
75 mm
2000 mm
274.66 mm
762 mm
Cell B
850.9 mm
25 mm
234.66 mm
Grade: 2.0%
75 mm
2000 mm
333.9 mm
812.8 mm
Cell C
25 mm
762 mm
293.9 mm
Grade: 2.0%
75 mm
2000 mm
314.26 mm
787.4 mm
Cell D
25 mm
774.5 mm
274.26 mm
Grade: 2.0%
75 mm
Project:
UVIC Bioretention
Date:
April 29 2014
Scale:
1:36
03
PRODUCED BY AN AUTODESK EDUCATIONAL PRODUCT

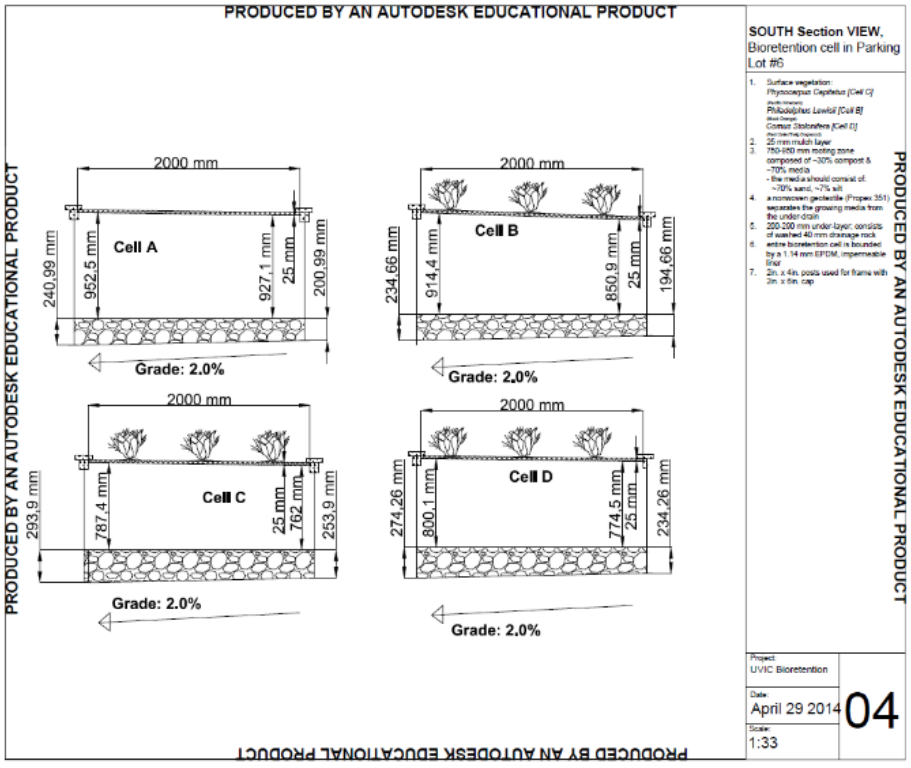
PRODUCED BY AN AUTODESK EDUCATIONAL PRODUCT
SOUTH Section VIEW,
Bioretention cell in Parking Lot #6
1. Surface vegetation:
Physocarpus Capitatus [Cell C]
Rhododphus Lawtoli [Cell B]
Cornus Stolonifera [Cell D]
2. 25 mm mulch layer
3. 750-950 mm rooting zone composed of ~30% compost & ~70% media
- the media should consist of: ~80% sand, ~2% silt
4. a nonwoven geotextile (Propex 351) separates the growing media from the underdrain
5. 200-200 mm under-layer: consists of washed 40 mm drainage rock
6. entire bioretention cell is bounded by a 1.14 mm EPDM, impermeable liner
7. 2in. x 4in. posts used for frame with 2in. x 6in. cap
PRODUCED BY AN AUTODESK EDUCATIONAL PRODUCT
2000 mm
240.99 mm
952.5 mm
Cell A
927.1 mm
25 mm
200.99 mm
Grade: 2.0%
2000 mm
234.66 mm
914.4 mm
Cell B
850.9 mm
25 mm
194.66 mm
Grade: 2.0%
2000 mm
293.9 mm
787.4 mm
Cell C
25 mm
762 mm
253.9 mm
Grade: 2.0%
2000 mm
274.26 mm
800.1 mm
Cell D
774.5 mm
25 mm
234.26 mm
Grade: 2.0%
Project:
UVIC Bioretention
Date:
April 29 2014
Scale:
1:33
04
PRODUCED BY AN AUTODESK EDUCATIONAL PRODUCT

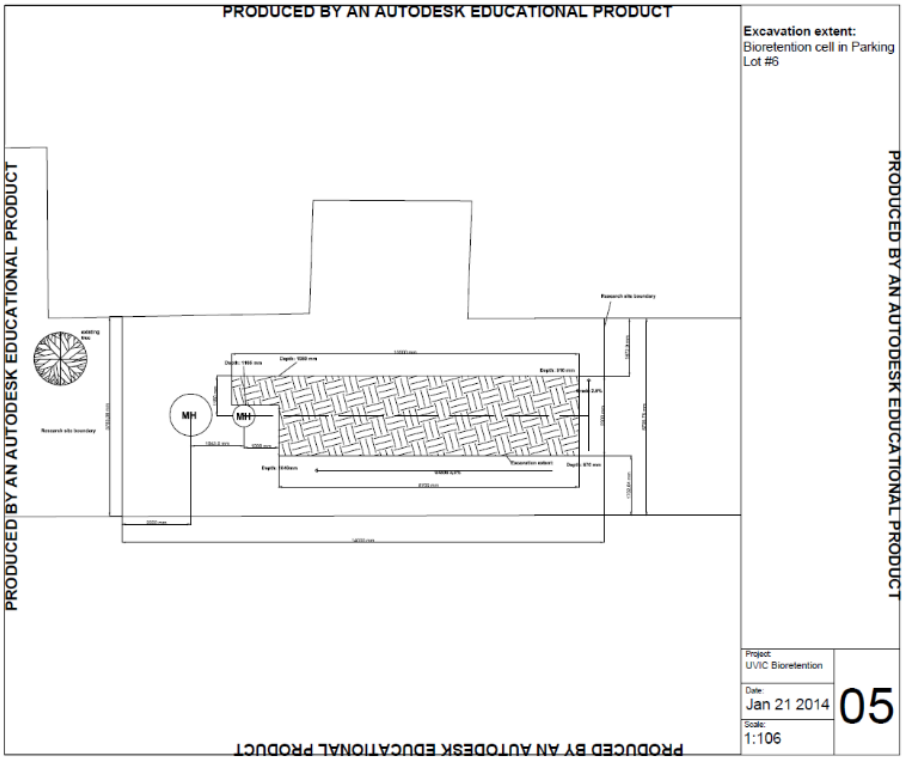
PRODUCED BY AN AUTODESK EDUCATIONAL PRODUCT
Excavation extent:
Bioretention cell in Parking Lot #6
PRODUCED BY AN AUTODESK EDUCATIONAL PRODUCT
MH
MH
Research site boundary
Project:
UVIC Bioretention
Date:
Jan 21 2014
Scale:
1:106
05
PRODUCED BY AN AUTODESK EDUCATIONAL PRODUCT

Appendix B – Test Volume Calculations

```
import glob
import numpy as np
import pandas as pd
import matplotlib.pyplot as plt

#Part 1: reading in, cleaning up, and orgainizing the data in a useful way.

#read in the daily data for 2009 - 2019 as a list and combine/convert to pandas dataframe, remove
# all undeeded data (only need to keep year, month and total precip - the dataset has much more).
#All in one line!!
df = pd.concat([pd.read_csv(f,usecols=['Year','Month','Total Precip (mm)'])
 for f in glob.glob(r'/Users/jessicadhami/Documents/School/MASc/Courses/GEOG524/Project/Data/*.csv')],
            ignore_index = True)

#Sebset each winetr: drop data for any month falling in the plant growing season (May to October)
#(Only keep data for plant senescence period), drop null values and drop month and year
#I will add

#note: The naming convention is by the year that that the senescence period started in,
#ie. winter of 2009-2010 is called 2009

#df_s=df.loc[(df['Month']<=4) | (df['Month']>=11)].dropna() - Realized I don't even need this intermediate dataset

df92=df.loc[(df['Month']>=11) & (df['Year']==1992)|(df['Month']<=4) & (df['Year']==1993)].dropna().drop(['Year', 'Month'], axis=1)
df93=df.loc[(df['Month']>=11) & (df['Year']==1993)|(df['Month']<=4) & (df['Year']==1994)].dropna().drop(['Year', 'Month'], axis=1)
df94=df.loc[(df['Month']>=11) & (df['Year']==1994)|(df['Month']<=4) & (df['Year']==1995)].dropna().drop(['Year', 'Month'], axis=1)
df95=df.loc[(df['Month']>=11) & (df['Year']==1995)|(df['Month']<=4) & (df['Year']==1996)].dropna().drop(['Year', 'Month'], axis=1)
df96=df.loc[(df['Month']>=11) & (df['Year']==1996)|(df['Month']<=4) & (df['Year']==1997)].dropna().drop(['Year', 'Month'], axis=1)
df97=df.loc[(df['Month']>=11) & (df['Year']==1997)|(df['Month']<=4) & (df['Year']==1998)].dropna().drop(['Year', 'Month'], axis=1)
df98=df.loc[(df['Month']>=11) & (df['Year']==1998)|(df['Month']<=4) & (df['Year']==1999)].dropna().drop(['Year', 'Month'], axis=1)
df99=df.loc[(df['Month']>=11) & (df['Year']==1999)|(df['Month']<=4) & (df['Year']==2000)].dropna().drop(['Year', 'Month'], axis=1)
df00=df.loc[(df['Month']>=11) & (df['Year']==2000)|(df['Month']<=4) & (df['Year']==2001)].dropna().drop(['Year', 'Month'], axis=1)
df01=df.loc[(df['Month']>=11) & (df['Year']==2001)|(df['Month']<=4) & (df['Year']==2002)].dropna().drop(['Year', 'Month'], axis=1)
df02=df.loc[(df['Month']>=11) & (df['Year']==2002)|(df['Month']<=4) & (df['Year']==2003)].dropna().drop(['Year', 'Month'], axis=1)
df03=df.loc[(df['Month']>=11) & (df['Year']==2003)|(df['Month']<=4) & (df['Year']==2004)].dropna().drop(['Year', 'Month'], axis=1)
df04=df.loc[(df['Month']>=11) & (df['Year']==2004)|(df['Month']<=4) & (df['Year']==2005)].dropna().drop(['Year', 'Month'], axis=1)
df05=df.loc[(df['Month']>=11) & (df['Year']==2005)|(df['Month']<=4) & (df['Year']==2006)].dropna().drop(['Year', 'Month'], axis=1)
df06=df.loc[(df['Month']>=11) & (df['Year']==2006)|(df['Month']<=4) & (df['Year']==2007)].dropna().drop(['Year', 'Month'], axis=1)
df07=df.loc[(df['Month']>=11) & (df['Year']==2007)|(df['Month']<=4) & (df['Year']==2008)].dropna().drop(['Year', 'Month'], axis=1)
df08=df.loc[(df['Month']>=11) & (df['Year']==2008)|(df['Month']<=4) & (df['Year']==2009)].dropna().drop(['Year', 'Month'], axis=1)
df09=df.loc[(df['Month']>=11) & (df['Year']==2009)|(df['Month']<=4) & (df['Year']==2010)].dropna().drop(['Year', 'Month'], axis=1)
df10=df.loc[(df['Month']>=11) & (df['Year']==2010)|(df['Month']<=4) & (df['Year']==2011)].dropna().drop(['Year', 'Month'], axis=1)
df11=df.loc[(df['Month']>=11) & (df['Year']==2011)|(df['Month']<=4) & (df['Year']==2012)].dropna().drop(['Year', 'Month'], axis=1)
df12=df.loc[(df['Month']>=11) & (df['Year']==2012)|(df['Month']<=4) & (df['Year']==2013)].dropna().drop(['Year', 'Month'], axis=1)
df13=df.loc[(df['Month']>=11) & (df['Year']==2013)|(df['Month']<=4) & (df['Year']==2014)].dropna().drop(['Year', 'Month'], axis=1)
df14=df.loc[(df['Month']>=11) & (df['Year']==2014)|(df['Month']<=4) & (df['Year']==2015)].dropna().drop(['Year', 'Month'], axis=1)
df15=df.loc[(df['Month']>=11) & (df['Year']==2015)|(df['Month']<=4) & (df['Year']==2016)].dropna().drop(['Year', 'Month'], axis=1)
df16=df.loc[(df['Month']>=11) & (df['Year']==2016)|(df['Month']<=4) & (df['Year']==2017)].dropna().drop(['Year', 'Month'], axis=1)
df17=df.loc[(df['Month']>=11) & (df['Year']==2017)|(df['Month']<=4) & (df['Year']==2018)].dropna().drop(['Year', 'Month'], axis=1)
df18=df.loc[(df['Month']>=11) & (df['Year']==2018)|(df['Month']<=4) & (df['Year']==2019)].dropna().drop(['Year', 'Month'], axis=1)

#Add a colum to identify the senesence period

df92['Year'] = 1992
df93['Year'] = 1993
df94['Year'] = 1994
df95['Year'] = 1995
df96['Year'] = 1996
df97['Year'] = 1997
df98['Year'] = 1998
df99['Year'] = 1999
df00['Year'] = 2000
df01['Year'] = 2001
df02['Year'] = 2002
df03['Year'] = 2003
df04['Year'] = 2004
```

```
df05['Year'] = 2005
df06['Year'] = 2006
df07['Year'] = 2007
df08['Year'] = 2008
df09['Year'] = 2009
df10['Year'] = 2010
df11['Year'] = 2011
df12['Year'] = 2012
df13['Year'] = 2013
df14['Year'] = 2014
df15['Year'] = 2015
df16['Year'] = 2016
df17['Year'] = 2017
df18['Year'] = 2018



#Make a new dataframe  of the annual senesence period max then reshape.

df_max = pd.concat([df92.max(), df93.max(),
                df94.max(), df95.max(), df96.max(), df97.max(), df98.max(),
                df99.max(), df00.max(), df01.max(), df02.max(), df03.max(),
                df04.max(), df05.max(), df06.max(), df07.max(), df08.max(),
                df09.max(), df10.max(), df11.max(), df12.max(), df13.max(),
                df14.max(), df15.max(), df16.max(), df17.max(), df18.max()])
df_max = pd.DataFrame(df_max.values.reshape(-1, 2), columns = ['Precip', 'Year'])



#Part 2: Complete frequency analysis of daily rain inensity

#Rank the new yearly datasets in decending order of precip


df_max['rank'] = df_max['Precip'].rank(ascending=0)

#compute exceedance probability p = (1/T) = rank/(m+1), where T is return period and m is number of observations
m=len(df_max)

df_max['p'] = df_max['rank']/(m+1)

#Work backwards to compute return period

df_max['T'] = 1/df_max['p']

#Sort in order of return period for ease of plotting

df_max_ordered = df_max.sort_values(by='T')

#Visualize the results, make sure the trends make sense
df_max_ordered.plot(x='T',y='Precip',logx=True)

df_max_ordered.plot.scatter(x='T',y='Precip', logx=True, xlim=(1,100))

plt.plot(df_max_ordered['T'], df_max_ordered['Precip'],'mo',label='Data')
plt.title("Frequency Analysis of Daily Rain Intensity")
plt.xlabel("Return Period [Years]")
plt.ylabel("Rainfall Intenisty [mm/day]")
plt.legend()

#Part 3: Apply non-linear regression to the results
# fitting a function of the form R=aT^b where R is intensity and T is return period.
from scipy.optimize import curve_fit

x=np.array(df_max_ordered['T'])
y=np.array(df_max_ordered['Precip'])

def func(x, a, b):
   return a*x**b
```

```
#original guesses are from excel

guess= [13.1,2.1]
c,cov = curve_fit(func, x, y,guess)

#coefficients for the equation of the power function
a=c[0]
b=c[1]

power_fit=a*df_max_ordered['T']+b

plt.plot(df_max_ordered['T'], df_max_ordered['Precip'],'mo',label='Data')
plt.plot(df_max_ordered['T'], power_fit,label='Regression Fit')
plt.title("Power Regression of Historical Rainfall Frequency")
plt.xlabel("Return Period [Years]")
plt.ylabel("Rainfall Intenisty [mm/day]")
plt.legend()
plt.annotate('R = $25.57 T ^{0.37}$',xy=(15,300))

#try again with an eponential funciton of the form R = d*ln(T)+e

def func2(x, d, e):
   return d*np.log(x)+e

#original guesses are from excel

g= [49,11]

f,fcov = curve_fit(func2, x, y,g)

#coefficients for the equation of the logarithimic function
d=f[0]
e=f[1]

ln_fit=d*np.log(df_max_ordered['T'])+e
plt.plot(df_max_ordered['T'], df_max_ordered['Precip'],'mo',label='Data')
plt.plot(df_max_ordered['T'], ln_fit,label='Regression Fit')
plt.title("Logarithmic Regression of Historical Rainfall Frequency (Seasonal Max)")
plt.xlabel("Return Period [Years]")
plt.ylabel("Rainfall Intenisty [mm/day]")
plt.legend()
plt.annotate('R = 19.07ln(T)+20.14',xy=(15,50))
```

Appendix C – SPSS Output for Wilcoxon Signed Ranks Test and Spearman's Rho Correlation

C.1 Wilcoxon Signed Ranks Test

Ranks

		N	Mean Rank	Sum of Ranks
DO_C - DO_B	Negative Ranks	1[a]	2.00	2.00
	Positive Ranks	8[b]	5.38	43.00
	Ties	0[c]		
	Total	9		
pH_C - pH_B	Negative Ranks	4[d]	4.50	18.00
	Positive Ranks	5[e]	5.40	27.00
	Ties	0[f]		
	Total	9		
COD_C - COD_B	Negative Ranks	0[g]	0.00	0.00
	Positive Ranks	9[h]	5.00	45.00
	Ties	0[i]		
	Total	9		
Total_P_C - Total_P_B	Negative Ranks	2[j]	4.50	9.00
	Positive Ranks	7[k]	5.14	36.00
	Ties	0[l]		
	Total	9		
Ortho_P_C - Ortho_P_B	Negative Ranks	1[m]	5.00	5.00
	Positive Ranks	8[n]	5.00	40.00
	Ties	0[o]		
	Total	9		
TSS_C - TSS_B	Negative Ranks	3[p]	3.33	10.00
	Positive Ranks	4[q]	4.50	18.00
	Ties	0[r]		
	Total	7		
TN_C - TN_B	Negative Ranks	4[s]	3.25	13.00
	Positive Ranks	5[t]	6.40	32.00

	Ties	0[u]		
	Total	9		
ToN_C - ToN_B	Negative Ranks	4[v]	6.00	24.00
	Positive Ranks	5[w]	4.20	21.00
	Ties	0[x]		
	Total	9		
NO3_N_C - NO3_N_B	Negative Ranks	1[y]	4.00	4.00
	Positive Ranks	8[z]	5.13	41.00
	Ties	0[aa]		
	Total	9		
Volume_C - Volume_B	Negative Ranks	1[ab]	1.00	1.00
	Positive Ranks	8[ac]	5.50	44.00
	Ties	0[ad]		
	Total	9		

a. DO_C < DO_B

b. DO_C > DO_B

c. DO_C = DO_B

d. pH_C < pH_B

e. pH_C > pH_B

f. pH_C = pH_B

g. COD_C < COD_B

h. COD_C > COD_B

i. COD_C = COD_B

j. Total_P_C < Total_P_B

k. Total_P_C > Total_P_B

l. Total_P_C = Total_P_B

m. Ortho_P_C < Ortho_P_B

n. Ortho_P_C > Ortho_P_B

o. Ortho_P_C = Ortho_P_B

p. TSS_C < TSS_B

q. TSS_C > TSS_B

r. TSS_C = TSS_B

s. TN_C < TN_B

t. TN_C > TN_B

u. TN_C = TN_B

v. ToN_C < ToN_B

w. ToN_C > ToN_B

x. ToN_C = ToN_B

y. NO3_N_C < NO3_N_B

z. NO3_N_C > NO3_N_B

aa. NO3_N_C = NO3_N_B

ab. Volume_C < Volume_B

ac. Volume_C > Volume_B

ad. Volume_C = Volume_B

	DO_C - DO_B	pH_C - pH_B	COD_C - COD_B	Total_P_C - Total_P_B	Ortho_P_C - Ortho_P_B	TSS_C - TSS_B	TN_C - TN_B	ToN_C - ToN_B	NO3_N_C - NO3_N_B	Volume_C - Volume_B
Z	-2.429[b]	-.533[b]	-2.666[b]	-1.599[b]	-2.073[b]	-.676[b]	-1.125[b]	-.178[c]	-2.192[b]	-2.549[b]
Asymp. Sig. (2-tailed)	0.015	0.594	0.008	0.110	0.038	0.499	0.260	0.859	0.028	0.011

a. Wilcoxon Signed Ranks Test

b. Based on negative ranks.

c. Based on positive ranks.

C.2 Spearman's Rho Correlation

Correlations – Bioretention Cells

			%Δ Volume Bioretention	ETc(mm/day)	Max T (C)	Average T (C)	Min T (C)	Max Wind(km/hr)	Average Wind (km/hr)	Max Humidity (%)	Average Humidity (%)	Min Humidity (%)	Max PAR (W/m^2)	Average PAR (W/m^2)
Spearman's rho	%Δ Volume Bioretention	Correlation Coefficient	1.000	.717*	.753*	.717*	.733*	0.385	.767*	-0.233	-0.283	-0.469	0.017	0.433
		Sig. (2-tailed)		0.030	0.019	0.030	0.025	0.306	0.016	0.546	0.460	0.203	0.966	0.244
		N	9	9	9	9	9	9	9	9	9	9	9	9
	ETc(mm/day)	Correlation Coefficient	.717*	1.000	0.661	.767*	.783*	0.552	.717*	-.783*	-.783*	-.929**	0.317	.917**
		Sig. (2-tailed)	0.030		0.053	0.016	0.013	0.123	0.030	0.013	0.013	0.000	0.406	0.001
		N	9	9	9	9	9	9	9	9	9	9	9	9
	Max T (C)	Correlation Coefficient	.753*	0.661	1.000	.929**	.937**	0.185	0.402	-0.402	-0.452	-0.592	-0.343	0.552
		Sig. (2-tailed)	0.019	0.053		0.000	0.000	0.634	0.284	0.284	0.222	0.093	0.366	0.123
		N	9	9	9	9	9	9	9	9	9	9	9	9
	Average T (C)	Correlation Coefficient	.717*	.767*	.929**	1.000	.933**	0.201	0.400	-0.583	-.667*	-.736*	-0.300	.700*
		Sig. (2-tailed)	0.030	0.016	0.000		0.000	0.604	0.286	0.099	0.050	0.024	0.433	0.036
		N	9	9	9	9	9	9	9	9	9	9	9	9
	Min T (C)	Correlation Coefficient	.733*	.783*	.937**	.933**	1.000	0.301	0.483	-0.550	-0.567	-.728*	-0.233	.700*

		Sig. (2-tailed)	0.025	0.013	0.000	0.000		0.431	0.187	0.125	0.112	0.026	0.546	0.036
		N	9	9	9	9	9	9	9	9	9	9	9	9
	Max Wind(km/hr)	Correlation Coefficient	0.385	0.552	0.185	0.201	0.301	1.000	0.661	-0.310	-0.351	-0.529	0.577	0.561
		Sig. (2-tailed)	0.306	0.123	0.634	0.604	0.431		0.053	0.417	0.354	0.143	0.104	0.116
		N	9	9	9	9	9	9	9	9	9	9	9	9
	Average Wind (km/hr)	Correlation Coefficient	.767*	.717*	0.402	0.400	0.483	0.661	1.000	-0.350	-0.367	-0.510	0.500	0.533
		Sig. (2-tailed)	0.016	0.030	0.284	0.286	0.187	0.053		0.356	0.332	0.160	0.170	0.139
		N	9	9	9	9	9	9	9	9	9	9	9	9
	Max Humidity (%)	Correlation Coefficient	-0.233	-.783*	-0.402	-0.583	-0.550	-0.310	-0.350	1.000	.967**	.929**	-0.383	-.933**
		Sig. (2-tailed)	0.546	0.013	0.284	0.099	0.125	0.417	0.356		0.000	0.000	0.308	0.000
		N	9	9	9	9	9	9	9	9	9	9	9	9
	Average Humidity (%)	Correlation Coefficient	-0.283	-.783*	-0.452	-.667*	-0.567	-0.351	-0.367	.967**	1.000	.929**	-0.300	-.933**
		Sig. (2-tailed)	0.460	0.013	0.222	0.050	0.112	0.354	0.332	0.000		0.000	0.433	0.000
		N	9	9	9	9	9	9	9	9	9	9	9	9
	Min Humidity (%)	Correlation Coefficient	-0.469	-.929**	-0.592	-.736*	-.728*	-0.529	-0.510	.929**	.929**	1.000	-0.326	-.996**
		Sig. (2-tailed)	0.203	0.000	0.093	0.024	0.026	0.143	0.160	0.000	0.000		0.391	0.000
		N	9	9	9	9	9	9	9	9	9	9	9	9

Max PAR (W/m^2)	Correlation Coefficient	0.017	0.317	-0.343	-0.300	-0.233	0.577	0.500	-0.383	-0.300	-0.326	1.000	0.367
	Sig. (2-tailed)	0.966	0.406	0.366	0.433	0.546	0.104	0.170	0.308	0.433	0.391		0.332
	N	9	9	9	9	9	9	9	9	9	9	9	9
Average PAR (W/m^2)	Correlation Coefficient	0.433	.917**	0.552	.700*	.700*	0.561	0.533	-.933**	-.933**	-.996**	0.367	1.000
	Sig. (2-tailed)	0.244	0.001	0.123	0.036	0.036	0.116	0.139	0.000	0.000	0.000	0.332	
	N	9	9	9	9	9	9	9	9	9	9	9	9

*. Correlation is significant at the 0.05 level (2-tailed).

**. Correlation is significant at the 0.01 level (2-tailed).

Correlations – Control Cells

			%Δ Volume Control	ETo(mm/day)	Max T (C)	Average T (C)	Min T (C)	Max Wind(km/hr)	Average Wind (km/hr)	Max Humidity (%)	Average Humidity (%)	Min Humidity (%)	Max PAR (W/m^2)	Average PAR (W/m^2)
Spearman's rho	%Δ Volume Control	Correlation Coefficient	1.000	0.184	0.218	0.200	0.183	-0.483	-0.233	-0.154	-0.083	-0.350	0.333	-0.067
		Sig. (2-tailed)		0.635	0.574	0.606	0.637	0.187	0.546	0.693	0.831	0.356	0.381	0.865
		N	9	9	9	9	9	9	9	9	9	9	9	9
	ETo(mm/day)	Correlation Coefficient	0.184	1.000	.908**	.895**	.753*	.669*	0.301	-.687*	-.870**	-.929**	0.569	.828**
		Sig. (2-tailed)	0.635		0.001	0.001	0.019	0.049	0.431	0.041	0.002	0.000	0.110	0.006
		N	9	9	9	9	9	9	9	9	9	9	9	9
	Max T (C)	Correlation Coefficient	0.218	.908**	1.000	.996**	.854**	0.644	0.293	-0.459	-.711*	-.862**	0.402	.711*
		Sig. (2-tailed)	0.574	0.001		0.000	0.003	0.061	0.444	0.214	0.032	0.003	0.284	0.032
		N	9	9	9	9	9	9	9	9	9	9	9	9
	Average T (C)	Correlation Coefficient	0.200	.895**	.996**	1.000	.867**	0.650	0.300	-0.436	-.683*	-.850**	0.367	.733*
		Sig. (2-tailed)	0.606	0.001	0.000		0.002	0.058	0.433	0.241	0.042	0.004	0.332	0.025
		N	9	9	9	9	9	9	9	9	9	9	9	9
	Min T (C)	Correlation Coefficient	0.183	.753*	.854**	.867**	1.000	0.650	0.367	-0.522	-.667*	-.733*	0.017	0.600
		Sig. (2-tailed)	0.637	0.019	0.003	0.002		0.058	0.332	0.150	0.050	0.025	0.966	0.088

	N	9	9	9	9	9	9	9	9	9	9	9	9
Max Wind(km/hr)	Correlation Coefficient	-0.483	.669*	0.644	0.650	0.650	1.000	0.533	-0.479	-.667*	-0.533	0.117	.717*
	Sig. (2-tailed)	0.187	0.049	0.061	0.058	0.058		0.139	0.192	0.050	0.139	0.765	0.030
	N	9	9	9	9	9	9	9	9	9	9	9	9
Average Wind (km/hr)	Correlation Coefficient	-0.233	0.301	0.293	0.300	0.367	0.533	1.000	0.026	-0.117	0.000	-0.333	0.167
	Sig. (2-tailed)	0.546	0.431	0.444	0.433	0.332	0.139		0.948	0.765	1.000	0.381	0.668
	N	9	9	9	9	9	9	9	9	9	9	9	9
Max Humidity (%)	Correlation Coefficient	-0.154	-.687*	-0.459	-0.436	-0.522	-0.479	0.026	1.000	.932**	.718*	-0.445	-.693*
	Sig. (2-tailed)	0.693	0.041	0.214	0.241	0.150	0.192	0.948		0.000	0.029	0.231	0.039
	N	9	9	9	9	9	9	9	9	9	9	9	9
Average Humidity (%)	Correlation Coefficient	-0.083	-.870**	-.711*	-.683*	-.667*	-.667*	-0.117	.932**	1.000	.850**	-0.517	-.783*
	Sig. (2-tailed)	0.831	0.002	0.032	0.042	0.050	0.050	0.765	0.000		0.004	0.154	0.013
	N	9	9	9	9	9	9	9	9	9	9	9	9
Min Humidity (%)	Correlation Coefficient	-0.350	-.929**	-.862**	-.850**	-.733*	-0.533	0.000	.718*	.850**	1.000	-.683*	-.783*
	Sig. (2-tailed)	0.356	0.000	0.003	0.004	0.025	0.139	1.000	0.029	0.004		0.042	0.013
	N	9	9	9	9	9	9	9	9	9	9	9	9
Max PAR (W/m^2)	Correlation Coefficient	0.333	0.569	0.402	0.367	0.017	0.117	-0.333	-0.445	-0.517	-.683*	1.000	0.500

		Sig. (2-tailed)	0.381	0.110	0.284	0.332	0.966	0.765	0.381	0.231	0.154	0.042		0.170
		N	9	9	9	9	9	9	9	9	9	9	9	9
	Average PAR (W/m^2)	Correlation Coefficient	-0.067	.828**	.711*	.733*	0.600	.717*	0.167	-.693*	-.783*	-.783*	0.500	1.000
		Sig. (2-tailed)	0.865	0.006	0.032	0.025	0.088	0.030	0.668	0.039	0.013	0.013	0.170	
		N	9	9	9	9	9	9	9	9	9	9	9	9

**. Correlation is significant at the 0.01 level (2-tailed).

*. Correlation is significant at the 0.05 level (2-tailed).

Appendix D – August Soil Moisture Data

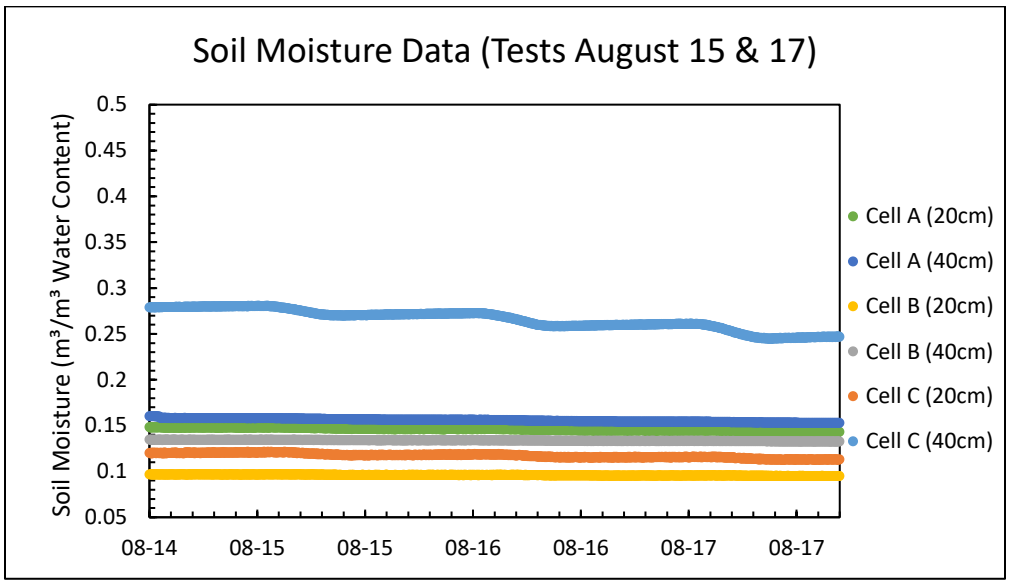

Figure 23. Soil moisture data for tests in August. Cell layout is provided in figure 2.